«ФИЗИКА ЭЛЕМЕНТАРНЫХ ЧАСТИЦ И АТОМНОГО ЯДРА»
2000, ТОМ 31, ВЫП. 4

539.143; 539.142.2; 539.21

GROUND STATE CORRELATIONS BEYOND RANDOM PHASE APPROXIMATION AND COLLECTIVE EXCITATIONS

V.V. Voronov[*], D. Karadjov*[**], F. Catara*[***], A.P. Severyukhin*[*]

1. INTRODUCTION 905
2. THE GENERAL SCHEME OF ERPA FOR SYSTEMS WITHOUT PAIRING 906
2.1. RPA Equations and Self-Consistency 907
2.2. One-Body and Two-Body Density Matrices 908
2.3. Extended Random Phase Approximation and Simplified Versions 911
2.4. An Application to Metallic Clusters 912
3. GROUND STATE CORRELATIONS AND QUASIPARTICLE PHONON MODEL 918
3.1. ERPA and the QPM Basic Formulae 918
3.2. GSC and Properties of Vibrational States 926
4. CONCLUSION 936
5. ACKNOWLEDGEMENTS 937
REFERENCES 937

[*] Joint Institute for Nuclear Research, Dubna
[**] Institute for Nuclear Research and Nuclear Energy, Sofia, Bulgaria
[***]Dipartimento di Fisica dell' Universita' and INFN, Catania, Italy

«ФИЗИКА ЭЛЕМЕНТАРНЫХ ЧАСТИЦ И АТОМНОГО ЯДРА»
2000, ТОМ 31, ВЫП. 4

539.143; 539.142.2; 539.21

GROUND STATE CORRELATIONS BEYOND RANDOM PHASE APPROXIMATION AND COLLECTIVE EXCITATIONS

V.V. Voronov[*], D. Karadjov*[**], F. Catara*[***], A.P. Severyukhin*[*]

We present a method which allows one to treat correlations in finite Fermi systems in a more consistent way than Random Phase Approximation (RPA). We derive a closed, nonlinear set of equations which determines the energies and wave-functions of the excited states as well as the single-particle occupation numbers in the ground state. As an example we apply it to metallic clusters. We show that our method allows one to correct for the inadequacy of standard RPA in cases where the use of quasiboson approximation becomes questionable. The basic equations of the nuclear quasiparticle-phonon model are generalized for the case when RPA phonons are replaced by the phonons of the extended RPA (ERPA). The properties of the low-lying vibrational states in spherical nuclei are studied within the developed approach.

Представлен метод, который позволяет трактовать корреляции в конечных ферми-системах более согласованным путем, чем в приближении случайных фаз (ПСФ). Получена замкнутая нелинейная система уравнений, которая определяет энергии и волновые функции возбужденных состояний, а также и одночастичные числа заполнения в основном состоянии. Приведен пример применения этой системы к исследованию металлических кластеров. Показано, что наш метод позволяет исправлять недостатки обычного ПСФ, когда использование квазибозонного приближения становится сомнительным. Основные уравнения квазичастично-фононной модели ядра обобщены на случай, когда фононы ПСФ заменяются на фононы расширенного ПСФ. В этом усовершенствованном подходе исследуются свойства низколежащих вибрационных состояний.

1. INTRODUCTION

The simplest theory of excited states of a quantum system where correlations in the ground state can be taken into account is the Random Phase Approximation (RPA). In this theory one introduces a set of operators Q_ν whose vacuum represents the ground state of the system, while the action of $Q_\nu^\dagger$ on this vacuum creates the excited states. Starting from a Hartree–Fock (HF) or a Hartree–Fock–Bogoliubov (HFB) state as a reference state to define single-particle levels, the $Q_\nu^\dagger$ operators are built as linear superpositions of particle-hole (p-h) or quasiparticle (qp) pair operators. The coefficients of these linear forms are solutions

[*] Joint Institute for Nuclear Research, Dubna
[**] Institute for Nuclear Research and Nuclear Energy, Sofia, Bulgaria
[***] Dipartimento di Fisica dell' Universita' and INFN, Catania, Italy

of equations which can be derived by using the equations-of-motion method [1]. If the Hamiltonian contains one- and two-body operators, the solution of these equations implies the evaluation of one- and two-body density matrices. In standard RPA, this difficulty is overcome by replacing the correlated ground state with the uncorrelated HF or HFB state whenever density matrices are needed. In the RPA equations there will appear expectation values of commutators of p-h or qp creation and annihilation operators and actually, the above approximation is equivalent to neglecting terms such that the commutators become those of boson operators. This is the origin of the name «quasiboson approximation» attached to this approximation.

The above remarks explain why possible improvements of RPA have been examined so far from two quite different points of view: either reformulating the whole theory in a boson formalism, paying attention to the violation of the Pauli principle [2], or remaining in the fermion space, attempting to eliminate as far as possible the above inconsistency [1, 3–16].

It is worth mentioning that renormalized RPA equations that include corrections for the ground state correlations (GSC) have been applied not only to the study of the properties of the low-lying isoscalar vibrations in spherical nuclei [11–13], but also to the investigation of the charge-exchange modes in nuclei [17–19] and the giant resonances in metal clusters [15, 16]. The GSC beyond RPA for nuclei at finite temperature have been considered in Refs. 20, 21.

In this work we follow the fermionic approach and we discuss an application of the extended RPA to describe collective excitations in metal clusters [15, 16] and spherical nuclei [13, 22]. We demonstrate that the basic equations of the Quasiparticle-Phonon-Model (QPM) developed by V.G.Soloviev and coauthors [23–26], where the RPA phonons are used as a basis, can be generalized to the ERPA case. Taking into account that the GSC beyond RPA results in a modification of the phonon-phonon coupling we study also the influence of such effects on properties of vibrational states in some spherical nuclei.

2. THE GENERAL SCHEME OF ERPA FOR SYSTEMS WITHOUT PAIRING

First of all we consider finite fermionic systems like metal clusters or atomic nuclei with closed shells where there is no pairing. The spirit of our method is close to that of Ref. 6 since we aim at using equations built with a correlated reference state $|0\rangle$ which is itself determined by these equations and therefore, the solution will be reached only after an iterative process.

Physical situation where ERPA can be necessary is found in clusters of atoms. In particular, recent RPA calculations based on jellium model for metallic clusters have shown [27, 28] that the values of occupation numbers in the ground state

can be rather different from the HF values, namely 0 and 1 for unoccupied and occupied single-particle states, respectively. This is just a case where the HF state does not resemble the correlated ground state and therefore, the standard RPA is clearly inconsistent and an improvement of the theory is required.

In this section we propose a generalization of standard RPA where ground state correlations are taken into account in a more consistent way. The formalism we are going to introduce goes one step further in the direction undertaken in previous papers [11, 14], where the Hara approach [3], and an improved version of it, were applied to the study of atomic nuclei.

2.1. RPA Equations and Self-Consistency. Let us denote by $|0\rangle$ the ground state of the system and by $|\nu\rangle$ its excited states, which are assumed to be linear combinations of p-h and hole-particle (h-p) configurations built upon $|0\rangle$

$$|\nu\rangle \equiv Q_\nu^\dagger|0\rangle \equiv \sum_{ph}[\psi_{ph}^\nu A_{ph}^\dagger - \phi_{ph}^\nu A_{ph}]|0\rangle \ , \tag{2.1}$$

where p (h) represents the quantum numbers of an unoccupied (occupied) single-particle state in the uncorrelated HF reference state $|HF\rangle$. In the above equation we have introduced renormalized p-h creation and annihilation operators

$$A_{ph}^\dagger = \sum_{p'h'} N_{ph,p'h'} a_{p'}^\dagger a_{h'} \ , \tag{2.2}$$

where the matrix N will be specified below. In order to avoid unnecessarily complicated expressions, we do not introduce coupling to total quantum numbers (angular momemtum,etc.) in the notations. By imposing that $|0\rangle$ is the vacuum for the Q_ν operators

$$Q_\nu|0\rangle = 0 \ , \tag{2.3}$$

the orthonormality conditions for the excited states read

$$\begin{aligned}
\delta_{\nu'\nu} \quad &= \langle\nu'|\nu\rangle = \langle 0|[Q_{\nu'}, Q_\nu^\dagger]|0\rangle \\
&= \sum_{ph,p'h'} \psi_{p'h'}^{\nu'*}\psi_{ph}^\nu \langle 0|[A_{p'h'}, A_{ph}^\dagger]|0\rangle + \phi_{p'h'}^{\nu'*}\phi_{ph}^\nu \langle 0|[A_{p'h'}^\dagger, A_{ph}]|0\rangle \\
&= \sum_{ph,p'h'} \sum_{p_1h_1,p_1'h_1'} N_{p'h',p_1h_1}^* N_{ph,p_1'h_1'} (\psi_{p'h'}^{\nu'*}\psi_{ph}^\nu - \phi_{ph}^{\nu'*}\phi_{p'h'}^\nu) \\
&\quad \times (\delta_{p_1p_1'}\langle 0|a_{h_1}^\dagger a_{h_1'}|0\rangle - \delta_{h_1h_1'}\langle 0|a_{p_1'}^\dagger a_{p_1}|0\rangle) \ .
\end{aligned} \tag{2.4}$$

If we assume for simplicity that the one-body density matrix is diagonal

$$\langle 0|a_\alpha^\dagger a_\beta|0\rangle = n_\alpha \delta_{\alpha\beta} \ , \tag{2.5}$$

and choose

$$N_{ph,p'h'} = \delta_{pp'}\delta_{hh'}(n_h - n_p)^{-1/2} \equiv \delta_{pp'}\delta_{hh'}D_{ph}^{-1/2} \ , \tag{2.6}$$

we obtain

$$\sum_{ph}(\psi_{ph}^{\nu'*}\psi_{ph}^{\nu} - \phi_{ph}^{\nu'*}\phi_{ph}^{\nu}) = \delta_{\nu\nu'} \ , \tag{2.7}$$

i.e., the same condition as in standard RPA. The same procedure was used in Ref. 1 to derive the «Renormalized RPA». The equations determining the amplitudes ψ and ϕ can be obtained by using the equations-of-motion method [1,29]. One gets

$$\begin{pmatrix} A & B \\ B^* & A^* \end{pmatrix}\begin{pmatrix} \psi^{\nu} \\ \phi^{\nu} \end{pmatrix} = E_{\nu}\begin{pmatrix} \psi^{\nu} \\ -\phi^{\nu} \end{pmatrix} \ , \tag{2.8}$$

where E_ν is the excitation energy of $|\nu\rangle$ and the matrices A and B have elements

$$A_{ph,p'h'} = \langle 0|\left[A_{ph}, H, A_{p'h'}^{\dagger}\right]|0\rangle \ , \tag{2.9}$$

and

$$B_{ph,p'h'} = -\langle 0|\left[A_{ph}^{\dagger}, H, A_{p'h'}^{\dagger}\right]|0\rangle \ , \tag{2.10}$$

H being the Hamiltonian of the system. In the above equations, the symmetrized double commutators are defined as

$$[A,B,C] = \frac{1}{2}\left\{[A,[B,C]] + [[A,B],C]\right\}. \tag{2.11}$$

As is apparent, equation (2.8) and the orthonormality condition (2.7) are formally identical to those of standard RPA, differing from the latters only in the fact that the elements of the matrices A and B contain the correlated ground state of the system rather than the HF one.

2.2. One-Body and Two-Body Density Matrices. We stress that Eqs. (2.7)–(2.10) are exact, within the space spanned by p-h and h-p elementary excitations. However, the evaluation of A and B matrix elements requires the knowledge of the one- and two-body density matrices. Here, we show that the one-body density matrix, and the p-h part of the two-body density matrix can be expressed exactly in terms of the ψ and ϕ amplitudes. Only the particle-particle and hole-hole parts of the two-body density matrix do not lend themselves easily to such expressions and for these parts we make an ansatz as explained below.

For the one-body density matrix, we use the number operator method [30] and find

$$n_h = 1 - \sum_{p\nu\nu'}[\delta_{\nu\nu'} - \frac{1}{2}\sum_{p'h'}D_{p'h'}\psi_{p'h'}^{\nu'}\psi_{p'h'}^{\nu*}]D_{ph}\phi_{ph}^{\nu}\phi_{ph}^{\nu'*} \ , \tag{2.12}$$

and

$$n_p = \sum_{h\nu\nu'} [\delta_{\nu\nu'} - \frac{1}{2} \sum_{p'h'} D_{p'h'} \psi^{\nu'}_{p'h'} \psi^{\nu *}_{p'h'}] D_{ph} \phi^{\nu}_{ph} \phi^{\nu' *}_{ph} \ . \tag{2.13}$$

The above expressions are exact up to terms $O(|\phi|^4)$.

Let us comment briefly these results. The occupation numbers of standard RPA, namely

$$n_h = 1 - \frac{1}{2} \sum_{p\nu} |\phi^{\nu}_{ph}|^2 \ , \tag{2.14}$$

and

$$n_p = \frac{1}{2} \sum_{h\nu} |\phi^{\nu}_{ph}|^2 \ , \tag{2.15}$$

are easily obtained by considering only terms up to $O(|\phi|^2)$ and approximating $D_{ph} \simeq 1$. The expressions for n_h and n_p of Eqs. (2.12) and (2.13) are also different, and more refined than those introduced in Refs. 3 and 14. In particular, in Ref. 14 an approximation suggested by boson mappings was used leading to

$$n_h = 1 - \sum_{p\nu} D_{ph} |\phi^{\nu}_{ph}|^2 \ , \tag{2.16}$$

and

$$n_p = \sum_{h\nu} D_{ph} |\phi^{\nu}_{ph}|^2 \ . \tag{2.17}$$

By maintaining only terms up to $O(|\phi|^2)$ in Eqs. (2.12) and (2.13) one gets expressions similar to those used in Ref. 14, differing from them by the factor $\frac{1}{2}$. It is interesting to remark that the same correction factor with respect to the standard RPA expressions [31] was found in Refs. 9, 30 many years ago. In conclusion, Eqs. (2.12) and (2.13) are definitely better than those derived and used in Ref. 14, at least because they tend continuously to the standard RPA expressions when the backward amplitudes ϕ are small.

We turn now to the part of the two-body density matrix containing at least one p-h pair. First, we invert Eq. (2.1) and its adjoint to express the operators $A^\dagger$ and A in terms of $Q^\dagger$ and Q:

$$A^\dagger_{ph} = \sum_{\nu} (\psi^{\nu *}_{ph} Q^\dagger_\nu + \phi^{\nu}_{ph} Q_\nu) \ , \tag{2.18}$$

$$A_{ph} = \sum_{\nu} (\psi^{\nu}_{ph} Q_\nu + \phi^{\nu *}_{ph} Q^\dagger_\nu) \ . \tag{2.19}$$

Using the above equations and (2.3) one easily finds

$$\langle 0 | a^\dagger_{p_1} a^\dagger_{h_2} a_{h_3} a_{h_4} | 0 \rangle = \langle 0 | a^\dagger_{h_1} a^\dagger_{p_2} a_{p_3} a_{p_4} | 0 \rangle = 0 \ . \tag{2.20}$$

Similarly one gets

$$\langle 0|a^\dagger_{p_1}a^\dagger_{h_2}a_{p_3}a_{h_4}|0\rangle = -\delta_{p_1p_3}\delta_{h_2h_4}n_{h_2} + D^{1/2}_{p_1h_4}D^{1/2}_{p_3h_2}\sum_\nu \psi^\nu_{p_3h_2}\psi^{\nu *}_{p_1h_4} \ , \quad (2.21)$$

and

$$\langle 0|a^\dagger_{p_1}a^\dagger_{p_2}a_{h_3}a_{h_4}|0\rangle = \frac{1}{2}[\langle 0|a^\dagger_{p_1}a^\dagger_{p_2}a_{h_3}a_{h_4}|0\rangle - \langle 0|a^\dagger_{p_2}a^\dagger_{p_1}a_{h_3}a_{h_4}|0\rangle] =$$

$$= \frac{1}{2}[D^{1/2}_{p_2h_3}D^{1/2}_{p_1h_4}\sum_\nu \phi^\nu_{p_2h_3}\psi^{\nu *}_{p_1h_4} - D^{1/2}_{p_1h_3}D^{1/2}_{p_2h_4}\sum_\nu \phi^\nu_{p_1h_3}\psi^{\nu *}_{p_2h_4}] \ . \quad (2.22)$$

The terms of the two-body density matrix we have considered so far have been expressed self-consistently in terms of the ψ and ϕ amplitudes. In order to calculate the remaining terms (of the particle-particle and hole-hole type), we have to introduce some approximation. We recall that

$$\langle HF|a^\dagger_{h_1}a^\dagger_{h_2}a_{h_3}a_{h_4}|HF\rangle = \delta_{h_1h_4}\delta_{h_2h_3} - \delta_{h_1h_3}\delta_{h_2h_4} \ , \quad (2.23)$$

and

$$\langle HF|a_{p_1}a_{p_2}a^\dagger_{p_3}a^\dagger_{p_4}|HF\rangle = \delta_{p_1p_4}\delta_{p_2p_3} - \delta_{p_1p_3}\delta_{p_2p_4} \ . \quad (2.24)$$

When the two-body density matrix is evaluated with respect to the correlated ground state $|0\rangle$ instead of $|HF\rangle$, the above equations are no longer valid. We propose to make the following diagonal ansatz:

$$\langle 0|a^\dagger_{h_1}a^\dagger_{h_2}a_{h_3}a_{h_4}|0\rangle = (\delta_{h_1h_4}\delta_{h_2h_3} - \delta_{h_1h_3}\delta_{h_2h_4})\langle 0|a^\dagger_{h_1}a^\dagger_{h_2}a_{h_2}a_{h_1}|0\rangle \ , \quad (2.25)$$

and

$$\langle 0|a^\dagger_{p_1}a^\dagger_{p_2}a_{p_3}a_{p_4}|0\rangle = (\delta_{p_1p_4}\delta_{p_2p_3} - \delta_{p_1p_3}\delta_{p_2p_4})\langle 0|a^\dagger_{p_1}a^\dagger_{p_2}a_{p_2}a_{p_1}|0\rangle \ . \quad (2.26)$$

With this ansatz the expressions (2.25), (2.26) reduce to the HF expressions (2.23), (2.24) when calculated in $|HF\rangle$, and they are manifestly antisymmetric. By using again the number operator method we calculate up to terms $O(|\phi|^4)$ the diagonal matrix elements in the r.h.s. of the above equations and obtain

$$\langle 0|a_{h_1}a_{h_2}a^\dagger_{h_2}a^\dagger_{h_1}|0\rangle = \frac{1}{2}\sum_{\nu\nu'}(\sum_{p'} D_{p'h_1}\psi^{\nu'}_{p'h_1}\psi^{\nu *}_{p'h_1})(\sum_p D_{ph_2}\phi^\nu_{ph_2}\phi^{\nu' *}_{ph_2}) \ , \quad (2.27)$$

$$\langle 0|a^\dagger_{p_1}a^\dagger_{p_2}a_{p_2}a_{p_1}|0\rangle = \frac{1}{2}\sum_{\nu\nu'}(\sum_{h'} D_{p_2h'}\psi^{\nu'}_{p_2h'}\psi^{\nu *}_{p_2h'})(\sum_h D_{p_1h}\phi^\nu_{p_1h}\phi^{\nu' *}_{p_1h}) \ . \quad (2.28)$$

In this way one can calculate the matrices A and B by expressing them in terms of the ψ and ϕ amplitudes. Therefore, Eqs. (2.8) become a set of nonlinear equations in the latter unknowns. They can be solved iteratively, starting from some initial guess for the ψ's and ϕ's and calculating with them A and B. The solution of Eqs. (2.8) gives a new set of ψ's and ϕ's, and so on until convergence is reached.

2.3. Extended Random Phase Approximation and Simplified Versions. As is well known, the RPA equations can also be obtained by linearizing the equations of motion [1]. All the elements of the two-body density matrix appearing in the commutator of the Hamiltonian with a p-h operator are contracted with respect to a reference state. In this way one obtains a quantity linear in the p-h operators. Substituting this in the double commutator of Eqs. (2.9), (2.10), one gets an expression for the matrices A and B containing only the one-body density matrix. When the reference state is chosen to be $|HF\rangle$, one obtains again the standard RPA. The generalization we propose, as a simplified version of the more general ERPA, is to use the same linearization method but choosing the correlated ground state $|0\rangle$ as reference state. Starting from Eqs. (2.9), (2.10) and performing the above described linearization procedure one gets

$$A_{ph,p'h'} = \frac{1}{2}(D_{ph}^{1/2} D_{p'h'}^{-1/2} + D_{p'h'}^{1/2} D_{ph}^{-1/2}) \times$$

$$\times \left\{ [(p'|t|p) + \sum_{\alpha} n_{\alpha}(p'\alpha|v|p\alpha)]\delta_{hh'} - [(h|t|h') + \sum_{\alpha} n_{\alpha}(\alpha h|v|\alpha h')]\delta_{pp'} \right\} +$$

$$+ D_{ph}^{1/2} D_{p'h'}^{1/2} (hp'|v|ph') \ , \tag{2.29}$$

and

$$B_{ph,p'h'} = D_{ph}^{1/2} D_{p'h'}^{1/2} (hh'|v|pp') \ , \tag{2.30}$$

where t is the kinetic-energy operator; and v, the two-body interaction. We solve the equations of motion (2.8) with the general expressions (2.29) and (2.30) for the matrix A and B in the basis diagonalizing the one-body density matrix. The latter is determined as follows. Following closely the number operator method [15] one can get in a generic basis

$$\langle 0|a_p^{\dagger} a_{p'}|0\rangle = \sum_{h\nu\nu'} \left[\delta_{\nu'\nu} - 1/2 \sum_{p_1 h_1} \langle 0|a_{h_1}^{\dagger} a_{p_1}|\Psi_{\nu'}\rangle \langle \Psi_{\nu}|a_{p_1}^{\dagger} a_{h_1}|0\rangle \right] \times$$

$$\times \langle 0|a_p^{\dagger} a_h|\Psi_{\nu}\rangle \langle \Psi_{\nu'}|a_h^{\dagger} a_{p'}|0\rangle \tag{2.31}$$

and

$$\langle 0|a_h^{\dagger} a_{h'}|0\rangle = \delta_{hh'} - \sum_{p\nu\nu'} \left[\delta_{\nu'\nu} - 1/2 \sum_{p_1 h_1} \langle 0|a_{h_1}^{\dagger} a_{p_1}|\Psi_{\nu'}\rangle \langle \Psi_{\nu}|a_{p_1}^{\dagger} a_{h_1}|0\rangle \right] \times$$

$$\times \langle 0|a_p^{\dagger} a_h|\Psi_{\nu}\rangle \langle \Psi_{\nu'}|a_{h'}^{\dagger} a_p|0\rangle \ , \tag{2.32}$$

which can be expressed in terms of the ψ and ϕ amplitudes and the matrix N using Eqs. (2.1), (2.2), and (2.3). In order to solve the so-obtained equations, we

use an iterative procedure and assume that at the nth iteration we can approximate the matrix N by using the diagonal form Eq. (2.6). We get then

$$\langle 0|a_p^\dagger a_{p_1}|0\rangle = \sum_{h\nu\nu'} \left[\delta_{\nu'\nu} - 1/2 \sum_{p'h'} D_{p'h'} \psi^{\nu'}_{p'h'} \psi^{\nu *}_{p'h'} \right] D^{1/2}_{ph} D^{1/2}_{p_1 h} \phi^{\nu}_{ph} \phi^{\nu' *}_{p_1 h} \quad (2.33)$$

and

$$\langle 0|a_h^\dagger a_{h_1}|0\rangle = \delta_{hh_1} - \sum_{p\nu\nu'} \left[\delta_{\nu'\nu} - 1/2 \sum_{p'h'} D_{p'h'} \psi^{\nu'}_{p'h'} \psi^{\nu *}_{p'h'} \right] D^{1/2}_{ph} D^{1/2}_{ph_1} \phi^{\nu}_{ph} \phi^{\nu' *}_{ph_1} \ , \quad (2.34)$$

where the occupation numbers in the right-hand sides (rhs) are approximate values at the nth iteration. By diagonalizing the matrices (2.33) and (2.34) one gets a new set of occupation numbers which are substituted in the rhs, and so on.

An essential simplification [15] can be done by neglecting the deviations from 0 and 1 of the occupation numbers appearing in the square brackets of Eq. (2.29), which then reduce to the HF single-particle energies ϵ_p and ϵ_h. The expression (2.29) of the matrix A simplifies then to

$$A_{ph,p'h'} = \delta_{pp'}\delta_{hh'}(\epsilon_p - \epsilon_h) + D^{1/2}_{ph} D^{1/2}_{p'h'} (hp'|v|ph') \ . \quad (2.35)$$

Equations (2.30) and (2.35) are identical to those used in Refs. 11, 14. However, the occupation numbers appearing in the coefficients D_{ph} as given by Eqs. (2.12), (2.13) are different from those of Refs. 11, 14 as discussed in the previous section. The above equations are also very similar to those proposed by Rowe [30] in his «Renormalized RPA». We see that the only difference with respect to standard RPA is the presence of the factor $D^{1/2}_{ph} D^{1/2}_{p'h'}$ which renormalizes the matrix elements of the residual interaction. Since these factors are less than or equal to unity, their effect will be to reduce the interaction matrix elements involving particle and hole states whose occupation numbers differ appreciably from the HF values.

Some recent applications of the above model (2.30), (2.35) with occupation numbers calculated as in Ref. 14, have shown that this quenching of the residual interaction plays an important role in the study of double β decay [32].

2.4. An Application to Metallic Clusters As the first example [15] for ERPA we apply the model (2.30), (2.35) with the occupation numbers (2.12), (2.13) to a specific example of metallic cluster.

Let us consider a metallic cluster consisting of N ions and N valence electrons. We assume for simplicity that the ionic background can be modelized by a jellium of constant density inside a sphere of radius $R = r_s N^{1/3}$, where r_s is

the Wigner–Seitz radius of the atoms:

$$n(r) = n_0\theta(R - r) \ . \tag{2.36}$$

The jellium produces an external field acting on the valence electrons:

$$V_{\rm ext}(\mathbf{r}) = -\int \frac{n(\mathbf{r}')}{|\mathbf{r} - \mathbf{r}'|} d^3r' \ . \tag{2.37}$$

The results will be expressed in eV and Å. The calculations are done for the cluster Na_{58} (r_s=3.93 a_0).

We have first solved the Hartree–Fock equations with a box boundary condition at a radius twice that of the jellium. We have then solved the standard RPA equations in the p-h configuration space, truncated so that for each multipolarity the Thouless theorem on EWSR is satisfied within 0.1%. Calculations have been done for excited states of total spin $S = 0$ and $S = 1$. It is known that, especially in the $S = 1$ channel, the screening of exchange interactions due to effects outside RPA is of paramount importance [33]. However, in order to study how much the more consistent treatment of ground state correlations in ERPA allows one to correct for the inadequacies of RPA, avoiding any confusion coming from possible double counting due to the use of a correlation term in the energy functional, we have decided to use the bare Coulomb interaction among electrons in the calculations we are going to discuss.

We examine first the occupation numbers and compare the RPA values, Eqs. (2.14), (2.15) with the ERPA ones, Eqs. (2.12), (2.13). In all cases we have considered states of multipolarities ranging from $L = 0$ to $L = 6$ in the summations appearing in those equations. When only the $S = 0$ degrees of freedom are included, the two sets of values are close to each other and to the HF limits, 0 and 1. This is shown in Fig. 1, where for the occupied states the quantities $(n_h - 1)$ rather n_h are reported in order to show in a clearer way the deviations. The situation is quite different when the $S = 1$ modes are also included. In the lower panel of Fig. 2 we see that now the RPA values deviate strongly from the HF limits, the maximum deviation being 0.32 for the last occupied single-particle state. The total number of electrons in the single-particle states below the Fermi level is 46.42. These findings clearly point to the fact that the quasi-boson approximation is not valid, and therefore standard RPA is not adequate, when both $S = 0$ and $S = 1$ channels are considered.

This conclusion was already reported in Ref. 15. The corresponding values obtained within ERPA are shown in the upper panel of the same Fig. 2. When ground state correlations are taken into account in a more consistent way, the occupation numbers turn out to be much closer to 0 and 1, with a maximum deviation equal to 0.15, and the total number of electrons below the Fermi level

is increased to 51.64. Therefore, we can say that RPA overestimates the correlations in the ground state and important modifications are introduced by the use of ERPA.

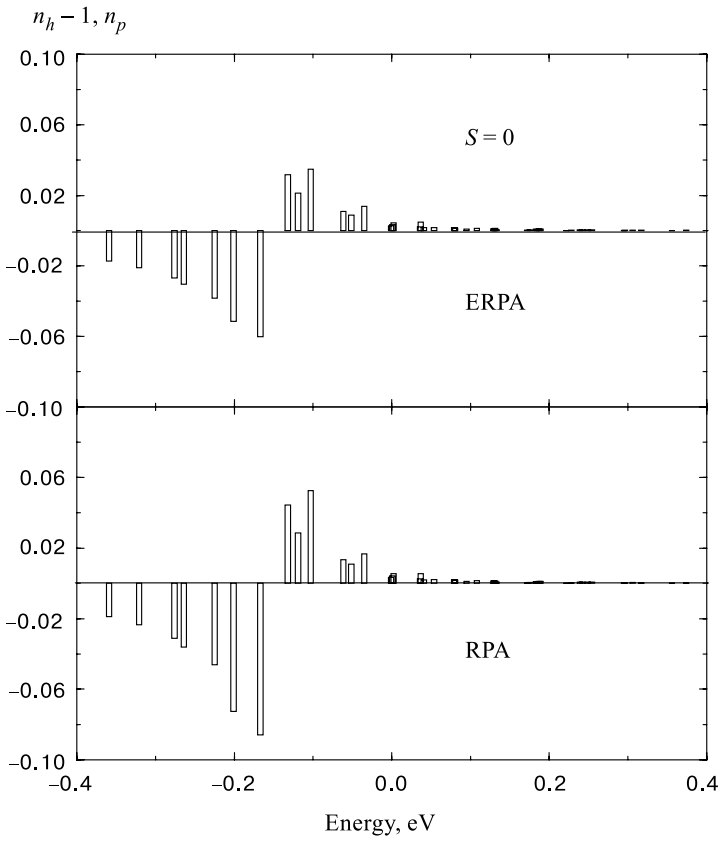

Fig. 1. Occupation numbers n_p for particle states and the opposite of depletion numbers $n_h - 1$ for hole states. In the lower and in the upper panel the RPA and ERPA results, respectively, are reported. Only spin $S = 0$ states are included in the calculations. In abscissa the single-particle energies in eV are indicated

The different sets of occupation numbers lead to the 3 electron densities $\rho(r)$ shown in Fig. 3, namely those calculated in HF, RPA and ERPA. The wiggles shown by the HF density in the interior part are smoothed when RPA correlations are included. In addition to that, the tail of the RPA density is much longer than the HF one. The ERPA density has a behaviour intermediate between the two

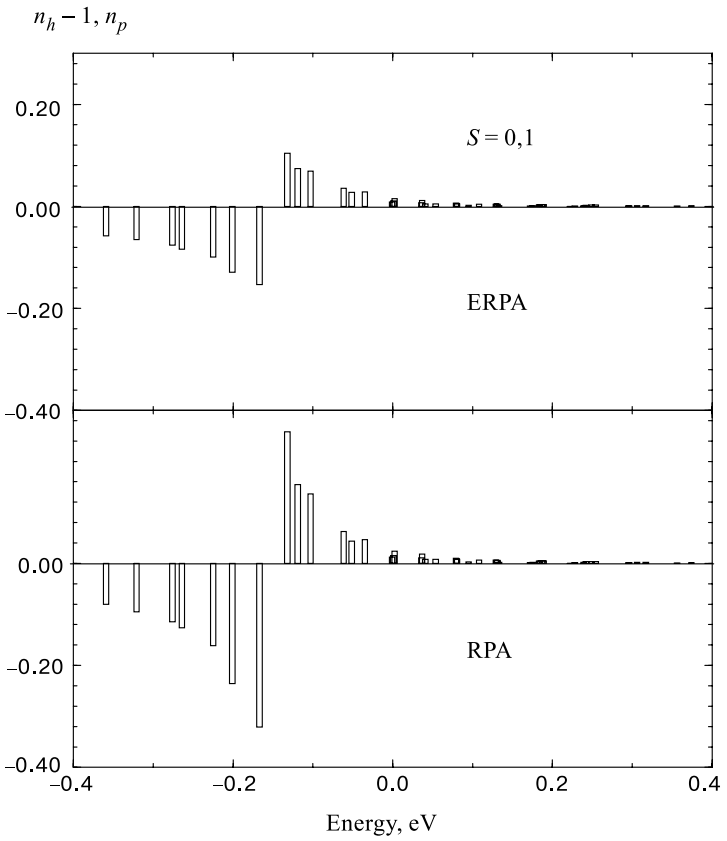

Fig. 2. As in Fig. 1, but including both $S = 0$ and $S = 1$ states

others. This difference is reflected in the electronic spillout

$$\Delta Z = 4\pi \int_R^\infty r^2 \rho(r) dr \tag{2.38}$$

which is 6.03, 8.94, and 7.85 respectively in the three approaches.

The more general method described in the previous section has been applied recently [16] to study the electronic properties of alkali metal clusters within the jellium approximation. For the interaction of the delocalized electrons with the ionic background and among themselves we use the bare Coulomb interaction rather than one derived from density functional including correlation terms. This choice is suggested by the fact that RPA and its generalizations explicitly include some correlations which, in principle, are also present in the density functional. Therefore, in order to avoid possible double countings, we prefer to use the bare

interaction. Its exchange parts are calculated exactly, without making local-density approximation.

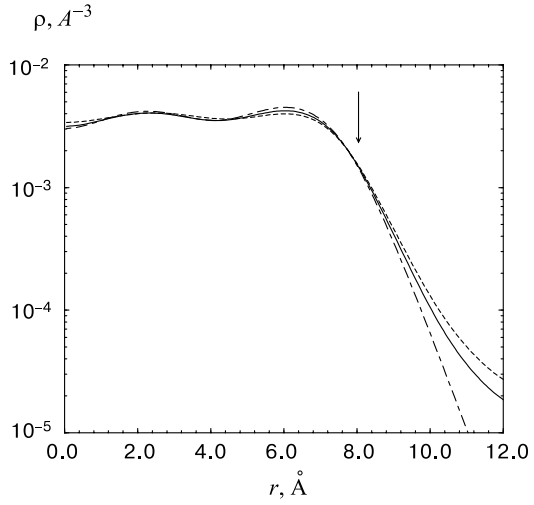

Fig. 3. Electron density ρ as obtained in HF (dot-dashed line), RPA (dotted line) and ERPA (full line). The arrow indicates the radius of the jellium sphere

First of all we solve the HF equations in order to fix the occupied and unoccupied single particle states, whose wave functions will be used as a zeroth order basis. Next we calculate the occupation numbers with an initial guess for the ψ and ϕ amplitudes. The best would be to make use of the coefficients, which result from the RPA equations. However, in some cases these equations are found to have imaginary solutions. This happens, for example, for some states with spin $S = 1$ and it is due to the fact that the bare Coloumb interaction is too much attractive in the $S = 1$ channel. The states having imaginary RPA energy are not included in this preliminary step. Then, we solve iteratively Eq. (2.8) with these values of the occupation numbers. Due to the fact that the interaction entering Eqs. (2.29) and (2.30) is quenched when the occupation numbers are different from 0 and 1, we find that the next solutions are real. With the new ψ and ϕ coefficients we can start the complete calculation which is again based on an iterative procedure. We compute the one-body density matrix, diagonalize it and recalculate the A and B matrices in the new basis. At this stage, the terms in curly brakets in Eq. (2.29) are also calculated correctly. Then we solve iteratively Eq. (2.8) in the new basis and with the new occupation numbers. The new set of ψ and ϕ is used to recalculate the one-body density matrix, which is again diagonalized and so on. The procedure is continued until the maximum difference in the occupation numbers between two successive iterations is less than a chosen limit. In the calculations we are going to present, this limit has been put equal to 10^{-6}.

In Fig. 4 we illustrate the $S = 0$ dipole strength distributions for the alkali clusters Na_N with $N = 8, 20, 40$, and 58. Solid lines refer to calculations performed within the present approach whereas dashed lines refer to standard RPA calculations. In all cases one observes an overall shift of the distributions to lower energies, as compared to the RPA results, while the basic structure of the

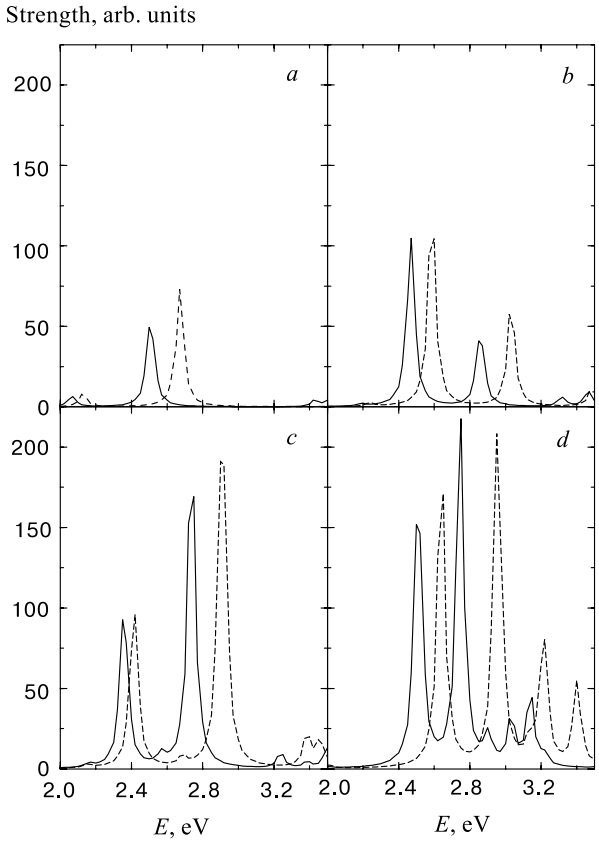

Fig. 4. $S = 0$ dipole strength distributions for the alkali clusters Na_N with $N = 8$ (*a*), 20 (*b*), 40 (*c*), and 58 (*d*). Solid lines refer to calculations performed within the present approach, whereas dashed lines refer to standard RPA calculations

distributions remains essentially unchanged. A comparison with the experimental photoabsorption cross sections turns out particulary useful. In the case of Na_8, the experimental distribution [34] exhibits a broad peak centered at about 2.5 eV, which is in good agreement with the plot of Fig. 4. A similar good agreement is observed in the case of Na_{20} where the experimental distribution [35] shows two broad peaks centered at about 2.4 and 2.8 eV, the first peak with a strength more than double the second one. Both in the case of Na_8 and Na_{20}, the shift produced by the present calculations with respect to the RPA ones improves the fit with experimental data.

The situation is less transparent in the case of Na_{40}. Here, in fact, the experimental distribution [35] exhibits two broad peaks at about 2.4 and 2.65 eV and the first one is higher than the second one. These data have to be compared with theoretical predictions which, in the present approach, shows two peaks at energy rather close to the experimental values (about 2.35 and 2.7 eV) but with the second one about twice the first one. The same situation occurs in the RPA case where, in addition, the energy of the second peak is found rather larger (about 2.9 eV). Therefore, the present calculations improve the RPA results for what concerns the energy of the peaks, but leave unsolved the problem of the relative height of the peaks.

3. GROUND STATE CORRELATIONS AND QUASIPARTICLE PHONON MODEL

The pairing is very important to describe properties of nuclei with open shells. To treat nuclear spectra one can replace the p-h pair operators $A^{\dagger}_{ph}$ and A_{ph} by the two-quasiparticle ones and in many cases the quasiparticle RPA is the basic method to treat the nuclear vibrational motion [26, 29, 36]. It is well known that due to the anharmonicity of vibrations there is a coupling between one-phonon and more complex states [26, 36]. Taking into account such a coupling it is possible to describe particularities of the low-lying states and damping of the giant resonances [23–26]. Usually such coupling was considered for the RPA phonons only [26].

In the present paper we use phonons of the extended RPA [12] as a basis on which the quasiparticle phonon model (QPM) [26] equations are generalized so as to account for the GSC in the description of nuclear vibrational states constructed by one- and two-phonon configurations. Besides the GSC, we take into account the Pauli principle corrections arising in the two-phonon terms due to the fermion structure of the phonon operators [37]. As an example we study the effect of the GSC on the energies, transition probabilities and transition densities of the low-lying vibrational states in Zn isotopes and compare present results with the results within other approaches.

3.1. ERPA and the QPM Basic Formulae. We employ the QPM Hamiltonian including an average nuclear field described as the Woods–Saxon potential, pairing interactions, the isoscalar and isovector particle–hole (p–h) and (p–p) residual forces in separable form with the Bohr–Mottelson radial dependence [36]:

$$H = \sum_{\tau} \left(\sum_{jm}{}^{\tau} (E_j - \lambda_\tau) a^{\dagger}_{jm} a_{jm} - \frac{1}{4} G^{(0)}_{\tau} : P^{\dagger}_0(\tau) P_0(\tau) : -
$$

$$\frac{1}{2}\sum_{a}\sum_{\sigma=\pm 1}\sum_{\lambda\mu}\left(\left(\kappa_0^{(\lambda,a)}+\sigma\kappa_1^{(\lambda,a)}\right):M_{\lambda\mu}^{(a)+}(\tau)M_{\lambda\mu}^{(a)}(\sigma\tau):\right). \quad (3.1)$$

We sum over the proton(p) and neutron(n) indexes and the notation $\{\tau = = (n,p)\}$ is used and a change $\tau \leftrightarrow -\tau$ means a change $p \leftrightarrow n$; a is the channel index $a = \{ph, pp\}$. The single-particle states are specified by the quantum numbers (jm); E_j are the single-particle energies; λ_τ is the chemical potential; $G_\tau^{(0)}$ and $\kappa^{(\lambda)}$ are the strengths in the p–p and in the p–h channel, respectively. The monopole pair creation and the multipole operators entering the normal products in (3.1) are defined as follows:

$$P_0^+ = \sum_{jm}(-1)^{j-m}a_{jm}^+a_{j-m}^+, \quad (3.2)$$

$$M_{\lambda\mu}^{(ph)+}(\tau) = \frac{1}{\sqrt{2\lambda+1}}\sum_{jj'mm'}{}^{\tau}(-1)^{j+m}\langle jmj'-m' \mid \lambda\mu\rangle f_{j'j}^{(\lambda)}a_{jm}^+a_{j'm'}, \quad (3.3)$$

$$M_{\lambda\mu}^{(pp)+}(\tau) = \frac{(-1)^{\lambda-\mu}}{\sqrt{2\lambda+1}}\sum_{jj'mm'}{}^{\tau}\langle jmj'm' \mid \lambda\mu\rangle f_{jj'}^{(\lambda)}a_{jm}^+a_{j'm'}^+, \quad (3.4)$$

where $f_{jj'}^{(\lambda)}$ are the single particle radial matrix elements of residual forces.

In what follows we work in quasiparticle (qp) representation, defined by the canonical Bogoliubov transformation:

$$a_{jm}^+ = u_j\alpha_{jm}^+ + (-1)^{j-m}v_j\alpha_{j-m}. \quad (3.5)$$

The Hamiltonian can be represented in terms of bifermion quasiparticle operators (and their conjugate ones):

$$B(jj';\lambda\mu) = \sum_{mm'}(-1)^{j'+m'}\langle jmj'm' \mid \lambda\mu\rangle\alpha_{jm}^+\alpha_{j'-m'}, \quad (3.6)$$

$$A^+(jj';\lambda\mu) = \sum_{mm'}\langle jmj'm' \mid \lambda\mu\rangle\alpha_{jm}^+\alpha_{j'm'}^+. \quad (3.7)$$

The phonon creation operators are defined in the 2-qp space in a standard fashion:

$$Q_{\lambda\mu,i}^+ = \frac{1}{2}\sum_{jj'}\{\psi_{jj'}^{\lambda i}\,A^+(jj';\lambda\mu) - (-1)^{\lambda-\mu}\varphi_{jj'}^{\lambda i}\,A(jj';\lambda-\mu)\}, \quad (3.8)$$

where the index $\lambda = 0, 1, 2, 3, ...$ denotes multipolarity and μ is its z projection in the laboratory system. The present definition of the phonon operators differs by a factor of 1/2 from (2.1) to keep the link with notations used in previous QPM papers. The following relation can be proved using the exact commutators of the fermion operators:

$$\langle 0 \mid [Q_{\lambda\mu,i}, Q^{+}_{\lambda'\mu',i'}] \mid 0\rangle = \frac{1}{2}\delta_{\lambda\lambda'}\delta_{\mu\mu'} \sum_{jj'} (1 - q_{jj'})[\psi^{\lambda i}_{jj'}\, \psi^{\lambda i'}_{jj'} - \varphi^{\lambda i}_{jj'}\varphi^{\lambda i'}_{jj'}], \tag{3.9}$$

where $\mid 0\rangle$ is the phonon vacuum, $q_{jj'} = q_j + q_{j'}$ and q_j is the quasiparticle distribution in the ground state: $q_j \equiv (2j+1)^{-\frac{1}{2}}\langle 0 \mid B(jj;00) \mid 0\rangle$. This relation corresponds to (2.4) if there is no pairing.

The pairing and phonon characteristics are determined by the following nonlinear system of equations [22]:

$$\frac{G^{(0)}_{\tau}}{2} \sum_{j}{}^{\tau} \frac{(j + 1/2)(1 - 2q_j)}{\sqrt{\Delta^2_{\tau} + (E_j - \lambda_{\tau})^2}} = 1, \tag{3.10}$$

$$N^{(\tau)} = \sum_{j}{}^{\tau} (j + 1/2)\left(1 - \frac{(E_j - \lambda_{\tau})\,(1 - 2q_j)}{\sqrt{\Delta^2_{\tau} + (E_j - \lambda_{\tau})^2}}\right), \tag{3.11}$$

$$\begin{pmatrix} M_0^{\kappa^{(\lambda,ph)}}(\tau) - I & M_1^{\kappa^{(\lambda,pp)}}(\tau) & M_2^{\kappa^{(\lambda,pp)}}(\tau) \\ M_1^{\kappa^{(\lambda,ph)}}(\tau) & M_4^{\kappa^{(\lambda,pp)}}(\tau) - I & M_3^{\kappa^{(\lambda,pp)}}(\tau) \\ M_2^{\kappa^{(\lambda,ph)}}(\tau) & M_3^{\kappa^{(\lambda,pp)}}(\tau) & M_5^{\kappa^{(\lambda,pp)}}(\tau) - I \end{pmatrix} \begin{pmatrix} D_0(\tau) \\ D_+(\tau) \\ D_-(\tau) \end{pmatrix} = 0, \tag{3.12}$$

$$\sum_{jj'} (1 - q_{jj'}) \left((\psi^{\lambda i}_{jj'})^2 - (\varphi^{\lambda i}_{jj'})^2\right) - 2 = 0, \tag{3.13}$$

$$q_j = \frac{1}{2}\sum_{\lambda i, j'} \frac{2\lambda + 1}{2j + 1}\,(1 - q_{jj'})\,(\varphi^{\lambda i}_{jj'})^2, \tag{3.14}$$

where

$$I = \begin{pmatrix} 1 & 0 \\ 0 & 1 \end{pmatrix}.$$

The formulae for the quasiparticle energies $\varepsilon_j = \sqrt{\Delta^2_{\tau} + (E_j - \lambda_{\tau})^2}$ and for the coefficients u_j, v_j remain the same as in the usual BCS theory; the new values for
$\Delta_{\tau} \equiv \frac{1}{2}G^{(0)}_{\tau}\sum_{j}^{(\tau)}(1-2q_j)(2j+1)u_j\,v_j$ and λ_{τ}, come from Eqs. (3.10) and (3.11); $\varepsilon_{jj'} = \varepsilon_j + \varepsilon_{j'}$.

We introduced the functions

$$D_n(\tau) = \begin{pmatrix} D_n^{\lambda i}(\tau) \\ D_n^{\lambda i}(-\tau) \end{pmatrix},$$

where $n = \{0, +, -\}$,

$$D_0^{\lambda i}(\tau) = \sum_{jj'}{}^{\tau} f_{jj'}^{(\lambda)}(1 - q_{jj'}) u_{jj'}^{(+)} \left(\psi_{jj'}^{\lambda i} + \varphi_{jj'}^{\lambda i}\right),$$

$$D_{\pm}^{\lambda i}(\tau) = \sum_{jj'}{}^{\tau} f_{jj'}^{(\lambda)}(1 - q_{jj'}) v_{jj'}^{(\pm)} \left(\psi_{jj'}^{\lambda i} \mp \varphi_{jj'}^{\lambda i}\right),$$

$v_{jj'}^{(\pm)} = u_j u_{j'} \pm v_j v_{j'}$, $u_{jj'}^{(\pm)} = u_j v_{j'} \pm v_j u_{j'}$.

The functions $M_l^{\kappa^{(\lambda,a)}}(\tau)$ have the following form

$$M_l^{\kappa^{(\lambda,a)}}(\tau) = \begin{pmatrix} (\kappa_0^{(\lambda,a)} + \kappa_1^{(\lambda,a)}) X_l^{\lambda\iota}(\tau) & (\kappa_0^{(\lambda,a)} - \kappa_1^{(\lambda,a)}) X_l^{\lambda\iota}(\tau) \\ (\kappa_0^{(\lambda,a)} - \kappa_1^{(\lambda,a)}) X_l^{\lambda\iota}(-\tau) & (\kappa_0^{(\lambda,a)} + \kappa_1^{(\lambda,a)}) X_l^{\lambda\iota}(-\tau) \end{pmatrix},$$

where

$l = \{0, 1, 2, 3, 4, 5\}$, $X_0^{\lambda i}(\tau) = \sum_{jj'}{}^{\tau} \mathcal{X}_{jj'}^{\lambda i} \left(u_{jj'}^{(+)}\right)^2 \varepsilon_{jj'}$,

$X_1^{\lambda i}(\tau) = \sum_{jj'}{}^{\tau} \mathcal{X}_{jj'}^{\lambda i} u_{jj'}^{(+)} v_{jj'}^{(+)} \omega_{\lambda i}$, $X_2^{\lambda i}(\tau) = \sum_{jj'}{}^{\tau} \mathcal{X}_{jj'}^{\lambda i} u_{jj'}^{(+)} v_{jj'}^{(-)} \varepsilon_{jj'}$,

$X_3^{\lambda i}(\tau) = \sum_{jj'}{}^{\tau} \mathcal{X}_{jj'}^{\lambda i} v_{jj'}^{(+)} v_{jj'}^{(-)} \omega_{\lambda i}$, $X_4^{\lambda i}(\tau) = \sum_{jj'}{}^{\tau} \mathcal{X}_{jj'}^{\lambda i} \left(v_{jj'}^{(+)}\right)^2 \varepsilon_{jj'}$,

$X_5^{\lambda i}(\tau) = \sum_{jj'}{}^{\tau} \mathcal{X}_{jj'}^{\lambda i} \left(v_{jj'}^{(-)}\right)^2 \varepsilon_{jj'}$,

$$\mathcal{X}_{jj'}^{\lambda i} = \frac{(f_{jj'}^{(\lambda)})^2 (1 - q_{jj'})}{(2\lambda + 1)\left(\varepsilon_{jj'}^2 - \omega_{\lambda i}^2\right)}.$$

One can get the following expressions for the phonon amplitudes:

$$\psi_{jj'}^{\lambda i}(\tau) = \frac{1}{\sqrt{2\mathcal{Y}_{\tau}^{\lambda i}}} \frac{f_{jj'}^{\lambda}}{\left(\varepsilon_{jj'} - \omega_{\lambda i}\right)} \left(u_{jj'}^{(+)} + v_{jj'}^{(+)} z_+^{\lambda i}(\tau) + v_{jj'}^{(-)} z_-^{\lambda i}(\tau)\right), \quad (3.15)$$

$$\varphi_{jj'}^{\lambda i}(\tau) = \frac{1}{\sqrt{2\mathcal{Y}_{\tau}^{\lambda i}}} \frac{f_{jj'}^{\lambda}}{\left(\varepsilon_{jj'} + \omega_{\lambda i}\right)} \left(u_{jj'}^{(+)} - v_{jj'}^{(+)} z_+^{\lambda i}(\tau) + v_{jj'}^{(-)} z_-^{\lambda i}(\tau)\right), \quad (3.16)$$

where

$$\mathcal{Y}_{\tau}^{\lambda i} = \frac{2\left(2\lambda+1\right)^{2}}{\left(D_{0}^{\lambda i}\left(\tau\right)\left(\kappa_{0}^{(\lambda,ph)}+\kappa_{1}^{(\lambda,ph)}\right)+D_{0}^{\lambda i}\left(-\tau\right)\left(\kappa_{0}^{(\lambda,ph)}-\kappa_{1}^{(\lambda,ph)}\right)\right)^{2}}, \quad (3.17)$$

$$z_{n}^{\lambda i}\left(\tau\right) = \frac{D_{n}^{\lambda i}\left(\tau\right)\left(\kappa_{0}^{(\lambda,pp)}+\kappa_{1}^{(\lambda,pp)}\right)+D_{n}^{\lambda i}\left(-\tau\right)\left(\kappa_{0}^{(\lambda,pp)}-\kappa_{1}^{(\lambda,pp)}\right)}{D_{0}^{\lambda i}\left(\tau\right)\left(\kappa_{0}^{(\lambda,ph)}+\kappa_{1}^{(\lambda,ph)}\right)+D_{0}^{\lambda i}\left(-\tau\right)\left(\kappa_{0}^{(\lambda,ph)}-\kappa_{1}^{(\lambda,ph)}\right)}, \quad (3.18)$$

and $n = \{+,-\}$.

The pairing vibrations ($\lambda = 0$) have been considered in [38]. The system of nonlinear ERPA equations (3.10)–(3.14) includes effects of the isoscalar and isovector forces in the p-h and p-p channels and it is a generalization of equations derived in [3, 11, 12]. This system treats the GSC self-consistently and describes the coupling between different vibrations, different phonon roots of a certain multipolarity and the pairing. Eq. (3.14) corresponds to Eq. (2.13) from the previous section. The factors $(1 - q_{jj'})$, distinguishing the new equations from the conventional BCS and RPA ones, take into account the blocking effect due to the Pauli principle. If we put $q_{jj'} = 0$ in the r.h.s. of Eq. (3.14), we get the expression for the quasiparticle distribution in the ground state in the RPA case [9, 30] (see (2.15)). In the case of q_j=0 equations (3.10)–(3.14) reduce to the usual BCS and RPA equations with the p-h and p-p channels [23, 26].

The GSC affect not only the RPA, but they also should change the quasiparticle-phonon coupling. To take into account such effects we follow the basic ideas of the QPM. Hereafter we derive the generalized QPM equations which take into account the GSC beyond the RPA. As it was shown in our previous paper [38] the pairing vibrations give a negligible contribution to q_j. On the other hand, the two-phonon configurations including the pairing vibration phonons have an energy essentially higher than the configurations constructed from usual vibration phonons. That is why we do not take into account the coupling with the pairing vibrations in what follows. Using the completeness and orthogonality conditions for the phonon operators one can express bifermion operators A^{+} and A by phonons:

$$A^{+}(jj';\lambda\mu) + (-)^{\lambda-\mu}A(jj';\lambda-\mu) = (1 - q_{jj'})\sum_{i}(\psi_{jj'}^{\lambda i} + \phi_{jj'}^{\lambda i})(Q_{\lambda\mu i}^{+} + (-)^{\lambda-\mu}Q_{\lambda-\mu i}). \quad (3.19)$$

The initial Hamiltonian (3.1) can be rewritten in terms of quasiparticle and phonon operators in the following form:

$$H \;=\; h_0 \;+\; h_0^{pp} \;+\; h_{QQ} \;+\; h_{QB}, \tag{3.20}$$

$$h_0 \;+\; h_0^{pp} \;=\; \sum_{jm} \varepsilon_j \, \alpha_{jm}^{+} \, \alpha_{jm}, \tag{3.21}$$

$$h_{QQ} = -\frac{1}{4} \sum_{\lambda\mu ii'\tau} \frac{\overline{X}^{\lambda ii'}(\tau) + \overline{X}^{\lambda i'i}(\tau)}{\sqrt{\mathcal{Y}_\tau^{\lambda i} \mathcal{Y}_\tau^{\lambda i'}}} Q_{\lambda\mu i}^{+} Q_{\lambda\mu i'}, \tag{3.22}$$

$$\begin{aligned} h_{QB} \;\;=\;\; & -\frac{1}{2\sqrt{2}} \sum_{\lambda\mu i\tau} \sum_{jj'}{}^{\tau} \frac{f_{jj'}^{(\lambda)}}{\sqrt{\mathcal{Y}_\tau^{\lambda i}}} \Big((-)^{\lambda-\mu} Q_{\lambda\mu i}^{+} L_{jj'}^{\lambda i(+)}(\tau) + \\ & Q_{\lambda-\mu i} L_{jj'}^{\lambda i(-)}(\tau) \Big) B(jj';\lambda-\mu) + h.c., \end{aligned}$$

where

$$\overline{X}^{\lambda ii'}(\tau) = \sqrt{\frac{\mathcal{Y}_\tau^{\lambda i}}{2}} \left(D_0^{\lambda i}(\tau) + D_+^{\lambda i}(\tau) \, z_+^{\lambda i'}(\tau) + D_-^{\lambda i}(\tau) \, z_-^{\lambda i'}(\tau) \right),$$

$$L_{jj'}^{\lambda i(\pm)}(\tau) = v_{jj'}^{(-)} + \left(z_-^{\lambda i}(\tau) \pm z_+^{\lambda i}(\tau) \right) \left(u_{jj'}^{(-)} - u_{jj'}^{(+)} \right).$$

One can prove that the solutions of the system of equations (3.10)–(3.14) obey the following equality:

$$\langle \, Q_{\lambda\mu i} \;|\; H \;|\; Q_{\lambda\mu i}^{+} \rangle \;=\; \omega_{\lambda i}. \tag{3.23}$$

The term h_{QB} is responsible for the mixing of the configurations and, therefore, for the description of many characteristics of the excited states of even–even nuclei. In the simplest case the wave functions of those states could be written down as:

$$\Psi_\nu(\lambda\mu) = \{ \sum_i R_i(\lambda\nu) Q_{\lambda\mu i}^{+} + \sum_{\lambda_1 i_1 \lambda_2 i_2} P_{\lambda_1 i_1}^{\lambda_2 i_2}(\lambda\nu) \left[Q_{\lambda_1\mu_1 i_1}^{+} Q_{\lambda_2\mu_2 i_2}^{+} \right]_{\lambda\mu} \} |0\rangle \tag{3.24}$$

with the normalization condition:

$$\begin{aligned} & \langle \Psi_\nu(JM) \;|\; \Psi_\nu(JM) \rangle = \sum_i R_i^2(J\nu) + \\ & 2 \sum_{\lambda_1 i_1 \lambda_2 i_2} (P_{\lambda_2 i_2}^{\lambda_1 i_1}(J\nu))^2 (1 + K^J(\lambda_1 i_1, \lambda_2 i_2)) = 1, \end{aligned} \tag{3.25}$$

where

$$K^J(\lambda_1 i_1, \lambda_2 i_2) \equiv K^J(\lambda_1 i_1, \lambda_2 i_2 \mid \lambda_2 i_2, \lambda_1 i_1)$$

and

$$K^J(\lambda_2 i_2, \lambda i' \mid \lambda i, \lambda_2 i_2) = (2\lambda+1)(2\lambda_2+1)\frac{1}{1+\delta_{i,i'}\delta_{\lambda i,\lambda_2 i_2}} \times$$
$$\sum_{j_1 j_2 j_3 j_4} (1 - \frac{1}{2} q_{j_1 j_2 j_3 j_4})(-1)^{j_2+j_4+J} \left\{ \begin{array}{ccc} j_1 & j_2 & \lambda_2 \\ j_4 & j_3 & \lambda \\ \lambda & \lambda_2 & J \end{array} \right\} \times$$
$$(\psi^{\lambda i'}_{j_1 j_4} \psi^{\lambda i}_{j_3 j_4} \psi^{\lambda_2 i_2}_{j_3 j_2} \psi^{\lambda_2 i_2}_{j_1 j_2} - \varphi^{\lambda_2 i_2}_{j_3 j_2} \varphi^{\lambda_2 i_2}_{j_1 j_2} \varphi^{\lambda i'}_{j_3 j_4} \varphi^{\lambda i}_{j_1 j_4}), \qquad (3.26)$$

$$q_{j_1 j_2 j_3 j_4} \equiv q_{j_1} + q_{j_2} + q_{j_3} + q_{j_4}.$$

The mean value of H is

$$\langle \Psi_\nu(JM) \mid H \mid \Psi_\nu(JM) \rangle = \sum_i R_i^2(J\nu)\omega_{Ji} + 2 \sum_{\lambda_1 i_1 \lambda_2 i_2} (P^{\lambda_1 i_1}_{\lambda_2 i_2}(J\nu))^2 \times$$
$$\times (\omega_{\lambda_1 i_1} + \omega_{\lambda_2 i_2} + \Delta\omega^J(\lambda_1 i_1, \lambda_2 i_2))(1 + K^J(\lambda_1 i_1, \lambda_2 i_2)) +$$
$$+2 \sum_{\lambda_1 i_1, i \lambda_2 i_2} R_i(J\nu) P^{\lambda_1 i_1}_{\lambda_2 i_2}(J\nu) U^{\lambda_1 i_1}_{\lambda_2 i_2}(J\nu)(1 + K^J(\lambda_1 i_1, \lambda_2 i_2)), \qquad (3.27)$$

where the matrix element coupling of one- and two-phonon configurations is:

$$\langle Q_{J\nu} | h_{QB} | \left[Q^+_{\lambda_1 i_1} Q^+_{\lambda_2 i_2} \right]_J \rangle = U^{\lambda_1 i_1}_{\lambda_2 i_2}(J\nu)(1 + K^J(\lambda_1 i_1, \lambda_2 i_2)), \qquad (3.28)$$

$$U^{\lambda_1 i_1}_{\lambda_2 i_2}(\lambda i) = (-1)^{\lambda_1+\lambda_2+\lambda} U^{\lambda_2 i_2}_{\lambda_1 i_1}(\lambda i),$$

$$U^{\lambda_1 i_1}_{\lambda_2 i_2}(\lambda i) \equiv \sum_\tau U^{\lambda_1 i_1}_{\lambda_2 i_2}(\lambda i, \tau),$$

$$U^{\lambda_1 i_1}_{\lambda_2 i_2}(\lambda i, \tau) = (-1)^{\lambda_1+\lambda_2+\lambda} \frac{1}{\sqrt{2}} \sqrt{(2\lambda_1+1)(2\lambda_2+1)} \sum_{j_1 j_2 j_3}{}^\tau (1 - q_{j_2 j_3}) \times$$
$$\times \left(\frac{f^\lambda_{j_1 j_2}}{\sqrt{\mathcal{Y}^{\lambda i}_\tau}} \left\{ \begin{array}{ccc} \lambda_1 & \lambda_2 & \lambda \\ j_2 & j_1 & j_3 \end{array} \right\} \left(\mathcal{L}^{\lambda i}_{j_1 j_2}(\tau) \psi^{\lambda_2 i_2}_{j_2 j_3} \phi^{\lambda_1 i_1}_{j_3 j_1} + \mathcal{L}^{\lambda i}_{j_2 j_1}(\tau) \psi^{\lambda_1 i_1}_{j_3 j_1} \phi^{\lambda_2 i_2}_{j_2 j_3} \right) +$$
$$+ \frac{f^{\lambda_1}_{j_1 j_2}}{\sqrt{\mathcal{Y}^{\lambda_1 i_1}_\tau}} \left\{ \begin{array}{ccc} \lambda_1 & \lambda_2 & \lambda \\ j_3 & j_2 & j_1 \end{array} \right\} \left(\mathcal{L}^{\lambda_1 i_1}_{j_2 j_1}(\tau) \phi^{\lambda_2 i_2}_{j_3 j_1} \phi^{\lambda i}_{j_2 j_3} + \mathcal{L}^{\lambda_1 i_1}_{j_1 j_2}(\tau) \psi^{\lambda i}_{j_2 j_3} \psi^{\lambda_2 i_2}_{j_3 j_1} \right) +$$

$$+\frac{f^{\lambda_2}_{j_1j_2}}{\sqrt{\mathcal{Y}^{\lambda_2 i_2}_{\tau}}}\left\{\begin{array}{ccc}\lambda_1 & \lambda_2 & \lambda\\ j_1 & j_3 & j_2\end{array}\right\}\left(\mathcal{L}^{\lambda_2 i_2}_{j_1 j_2}(\tau)\,\phi^{\lambda_1 i_1}_{j_2 j_3}\phi^{\lambda i}_{j_3 j_1}+\mathcal{L}^{\lambda_2 i_2}_{j_2 j_1}(\tau)\,\psi^{\lambda i}_{j_3 j_1}\psi^{\lambda_1 i_1}_{j_2 j_3}\right)\Bigg)$$

$$\mathcal{L}^{\lambda i}_{j_1 j_2}(\tau)=\frac{1}{2}\left(L^{\lambda i(+)}_{j_1 j_2}+L^{\lambda i(-)}_{j_2 j_1}\right)$$

and

$$\Delta\omega^J(\lambda_1 i_1,\lambda_2 i_2)=$$

$$=-\frac{1}{4}\sum_{i\tau}\left(\frac{\overline{X}^{\lambda_1 i_1 i}(\tau)+\overline{X}^{\lambda i i_1}(\tau)}{\sqrt{\mathcal{Y}^{\lambda_1 i_1}_{\tau}\mathcal{Y}^{\lambda_1 i}_{\tau}}}K^J(\lambda_2 i_2,\lambda_1 i\mid\lambda_1 i_1,\lambda_2 i_2)+\right.$$

$$\left.+\frac{\overline{X}^{\lambda i_2 i}(\tau)+\overline{X}^{\lambda i i_2}(\tau)}{\sqrt{\mathcal{Y}^{\lambda_2 i_2}_{\tau}\mathcal{Y}^{\lambda_2 i}_{\tau}}}K^J(\lambda_2 i,\lambda_1 i_1\mid\lambda_1 i_1,\lambda_2 i_2)\right).$$

Calculating the mean value of H we used the so-called quasidiagonal approximation for the quantities $K^J(\lambda_1 i_1,\lambda_2 i_2\mid\lambda_3 i_3,\lambda_4 i_4)$ because the diagonal terms dominate over nondiagonal ones (see [26, 37]).

Using the variational principle in the form:

$$\delta\ \left(\langle\,\Psi_\nu(\lambda\mu)\,|H\mid\,\Psi_\nu(\lambda\mu)\rangle\ -\ E_\nu\left(\langle\,\Psi_\nu(\lambda\mu)\,|\,\Psi_\nu(\lambda\mu)\rangle\ -\ 1\right)\right)\ =\ 0 \qquad (3.29)$$

one obtains the following system of equations:

$$(\omega_{Ji}-E_\nu)R_i(J\nu)+\sum_{\lambda_1 i_1\lambda_2 i_2}P^{\lambda_1 i_1}_{\lambda_2 i_2}(J\nu)U^{\lambda_1 i_1}_{\lambda_2 i_2}(J\nu)(1+K^J(\lambda_1 i_1,\lambda_2 i_2))=0, \qquad (3.30)$$

$$2(\omega_{\lambda_1 i_1}+\omega_{\lambda_2 i_2}+\Delta\omega^J(\lambda_1 i_1,\lambda_2 i_2)-E_\nu)P^{\lambda_1 i_1}_{\lambda_2 i_2}(J\nu)+\sum_i R_i(J\nu)U^{\lambda_1 i_1}_{\lambda_2 i_2}(Ji)=0. \qquad (3.31)$$

The energies of the states (3.24) are solutions of

$$F(E_\nu)\equiv det\Bigg|(\omega_{\lambda i}-E_\nu)\delta_{ii'}-$$

$$-\frac{1}{2}\sum_{\lambda_1 i_1,\lambda_2 i_2}\frac{U^{\lambda_1 i_1}_{\lambda_2 i_2}(\lambda i)U^{\lambda_1 i_1}_{\lambda_2 i_2}(\lambda i')\left(1+K^J(\lambda_1 i_1,\lambda_2 i_2)\right)}{\omega_{\lambda_1 i_1}+\omega_{\lambda_2 i_2}+\Delta\omega^J(\lambda_1 i_1,\lambda_2 i_2)-E_\nu}\Bigg|=0. \qquad (3.32)$$

The rank of the determinant (3.32) is determined by the number of the one-phonon configurations included in the first term of the wave function (3.24).

These equations are more general in comparison with the ones derived for the pure p-h channel [13]. The equations derived above have the same form as

the basic QPM-equations [26, 37] and we call them the extended QPM with the Pauli principle corrections (EQPMPP) in what follows. The GSC affect phonon energies $\omega_{\lambda i}$, normalization constants $\mathcal{Y}_{\tau}^{\lambda i}$ and renormalize the matrix elements of the quasiparticle-phonon interaction. If we put $K^J(\lambda_1 i_1, \lambda_2 i_2) = 0$ we get the equations already derived in [39] where all the fourth-order terms in phonon amplitudes $\psi_{jj'}^{\lambda i}$ and $\phi_{jj'}^{\lambda i}$ were neglected (we call this approach the extended QPM (EQPM)). In the limit $q_{jj'} \to 0$ one reproduces precisely all the expressions of the QPM with taking into account the Pauli principle corrections [26, 37](QPMPP). In the case when $q_{jj'} = 0$ and $K^J(\lambda_1 i_1, \lambda_2 i_2) = 0$ we have equations describing coupling of one- and two-RPA phonons without taking into account the Pauli principle (QPM approach in the following discussions).

3.2. GSC and Properties of Vibrational States. The charge transition density, being the spatial overlap between the ground state wave function and the excited state wave function, provides a good test for nuclear models. The surface nature of the low-lying collective states predicted by calculations performed within the Hartree–Fock (HF) approach with effective forces [40] and the finite Fermi systems theory [41] has been demonstrated in the experiments on inelastic electron scattering from magic nuclei [42]. The changes of the nuclear densities due to the zero point fluctuations associated with surface modes in the Ca isotopes were calculated within the nuclear field theory in Ref. 43, where the quasiparticle distribution in the ground state was calculated within the RPA. Recent experimental and theoretical (based on the random phase approximation (RPA)) studies of the charge transition densities [44,45] of the low-lying states in some spherical nuclei are in reasonable agreement, but the theory gives too large fluctuations of the transition densities in the interior region. All theoretical calculations in RPA, as in HF, demonstrate the same behaviour in the nuclear interior, which indicates a systematic problem of a more fundamental nature (a detailed discussion can be found in Refs. 46, 47.

We study this long standing problem within our approach. Knowing the wave functions it is not difficult to calculate any matrix elements and physical quantities. For example, the charge transition density is calculated by the formula:

$$\rho_{\nu}^{(J)}(r) = \sum_{j_1 j_2} \rho_{j_1 j_2}^{J}(r) \{ \frac{1}{2}(1 - q_{j_1 j_2}) u_{j_1 j_2}^{(+)} \sum_{i} R_i(J\nu)(\psi_{j_1 j_2}^{Ji} + \phi_{j_1 j_2}^{Ji}) - v_{j_1 j_2}^{(-)} \sum_{\lambda_1 i_1 \lambda_2 i_2} \sqrt{(2\lambda_1+1)(2\lambda_2+1)} P_{\lambda_2 i_2}^{\lambda_1 i_1}(J\nu) \sum_{j_3} (1 - q_{j_3 j_1}) \times \left\{ \begin{array}{ccc} \lambda_1 & \lambda_2 & J \\ j_1 & j_2 & j_3 \end{array} \right\} (\psi_{j_2 j_3}^{\lambda_1 i_1} \phi_{j_3 j_1}^{\lambda_2 i_2} + \psi_{j_3 j_1}^{\lambda_2 i_2} \phi_{j_2 j_3}^{\lambda_1 i_1}) \}. \quad (3.33)$$

The expression for the two-quasiparticle transition density $\rho_{j_1 j_2}^{J}(r)$ can be found in [44]. Our charge-transition densities are folded with the formfactor of the

proton charge distribution [48]. Using quantities (3.33) one calculates the reduced transition probabilities from the ground to the excited state $(J\nu)$ [49]

$$B(EJ;0^+ \to (J\nu)) = (2J+1) \mid \int_0^\infty r^{J+2} \rho_\nu^{(J)}(r) dr \mid^2 . \qquad (3.34)$$

As an example we have performed numerical calculations for the Zn isotopes. The Woods–Saxon potential parameters in use are from [38], slightly modified to better describe the ground state density. In so far as our single-particle spectrum includes the bound and quasibound states we do not use any effective charge to calculate the electromagnetic transition probabilities. The pairing constants $G_\tau^{(0)}$ are fixed so as to reproduce the odd-even mass difference of neighbouring nuclei. As was shown in Ref. 22, the ERPA calculations with the p-p channel give results that are very close to the p-h ERPA ones and that is why we neglect the p-p channel in what follows. We give one example to demonstrate the influence of the p-p channel on the transition charge density later. The strength parameters $\kappa^{(\lambda)}$ for the cases based on the RPA and ERPA schemes are adjusted so that the $B(E\lambda)$ values calculated with the wave function (3.24) within both approaches are reasonably close to the experimental ones. This means that $\kappa^{(\lambda)}$ for the ERPA calculations are larger than for the RPA ones [12]. No changes of $\kappa^{(\lambda)}$ have been done for calculations without the two-phonon terms. We use the ratio $\kappa_1^{(\lambda)}/\kappa_0^{(\lambda)} = -1.2$ that enables one to reproduce the excitation energies of the isovector giant resonances in spherical nuclei. It is worth to mention that in our previous papers [11,12,38] we took into account only the isoscalar interaction for the p-h channel, but the inclusion of the isovector interaction does not affect the structure of low-lying states practically. It should be noted also that according to our present calculations the selfconsistent inclusion of the GSC in the pairing problem (see Eqs. (3.10)–(3.11)) guarantees the number conservation with a high accuracy, otherwise the deviation of the average particle number from the exact one reaches up to 3%.

The system of Eqs. (3.10)–(3.14) describes (via Eq. (3.14)) the coupling between different vibrations and between all the phonon roots of a certain multipolarity. Our studies [11] show that the interplay of different roots of the system of Eqs. (3.10)–(3.14) is not essential: the contribution from the second root for example affects the q_j by no more than 2 %. Thus, one can restrict the sum in Eq. (3.14) to only the first (collective) root without substantial loss of accuracy. According to our calculations for ^{64}Zn [11] the most essential role for the GSC is played by the quadrupole and octupole vibrations. The values of q_j calculated for the pure quadrupole vibrations (i.e. $\lambda = 2$, only) are as a rule a few times higher than those for the pure octupole vibrations ($\lambda = 3$, only). However, in the case of coupled ($\lambda = 2, 3$) vibrations the resulting q_j are larger than the sum of

q_j ($\lambda = 2$) and q_j ($\lambda = 3$) contrary to the RPA case because of the nonlinear character of the λ mixing. The admixture of the hexadecapole vibrations changes q_j by no more than 5 %. In addition we checked the effect of the inclusion of $\lambda = 5, 6$ terms for all the Zn isotopes. These terms do not affect the results, hence, one can take into account the mixing of the quadrupole and octupole modes only.

Solving the nonlinear equations (3.10)–(3.14) one can find the phonon amplitudes, energies and the quasiparticle distributions within ERPA. Making use of them as input values it is possible to define from equations (3.25), (3.30)–(3.32) the energies and the structure of the states described by the wave function (3.24).

Table 1. Quasiparticle distribution in the ground state of ^{68}Zn

	q_{nlj}			
	neutrons		protons	
nlj	RPA	ERPA	RPA	ERPA
$2s_{1/2}$	0.0047	0.0134	0.0122	0.0189
$1f_{7/2}$	0.0163	0.0222	0.0320	0.0451
$2p_{3/2}$	0.0540	0.0651	0.0862	0.1053
$1f_{5/2}$	0.0482	0.0609	0.0324	0.0445
$2p_{1/2}$	0.0899	0.0994	0.0359	0.0461
$1g_{9/2}$	0.0230	0.0295	0.0144	0.0161
$2d_{5/2}$	0.0072	0.0087	0.0042	0.0047

The results of our calculations for the quasiparticle distribution in the ground state of ^{68}Zn are shown in Table 1. It contains the values of q_j obtained in the RPA and ERPA schemes. As one can see from the table the q_j have large values for the subshells near the Fermi surface only and the ERPA gives stronger correlations in comparison with the RPA. A similar behaviour of q_j's has been found for other Zn isotopes [12]. This is valid for our choice of the multipole constants. As was mentioned above, the multipole constants $\kappa^{(\lambda,ph)}$ have been chosen to describe with a reasonable accuracy experimental $B(E\lambda)$-values. The value of $\kappa_0^{(2,ph)} = 0.0259$ MeV/fm for the nonlinear problem is quite larger than the critical RPA constant $\kappa_0^{(2,ph)} = 0.0242$ MeV/fm where the RPA solution becomes complex. (In the RPA case $\kappa_0^{(2,ph)} = 0.0227$ MeV/fm). The octupole constants in use are equal to $\kappa_0^{(3,ph)} = 0.0235$ MeV/fm for the RPA and $\kappa_0^{(3,ph)} = = 0.0250$ MeV/fm for the ERPA calculations, respectively. The last value is smaller than the critical RPA constant for the octupole vibrations in contrast to the quadrupole ones. The dependence of the 2_1^+ energies on $\kappa_0^{(2,ph)}$ at the fixed

value of $\kappa_0^{(3,ph)}$ in ^{64}Zn for the RPA and ERPA is presented in Fig. 5. It is seen from this figure that the ERPA has no critical point in contrast to the RPA case. Due to the coupling of the octupole vibrations with the quadrupole ones (via q_j) the first 3^- state loses its collectivity and the 3_1^- energy goes up. Such a behaviour is a consequence of the Pauli principle.

Taking into account the p-p channel results in some reduction of values of q_j, but not more than 8% and such a reduction does not change the transition charge densities (see Fig. 6). All the calculations based on the RPA phonons (RPA, QPM, QPMPP) have been performed with the RPA constants as well all the calculations based on the ERPA phonons (ERPA, EQPM, EQPMPP) have been done with the ERPA set of constants. It is worth mentioning that as in the case of metallic clusters ([15]) our ERPA calculation gives also weaker correlations compared to the RPA ones, if the same set of multipole constants is used in both approximations, but in this case neither energies nor transition probabilities can be reproduced within the ERPA or its modifications.

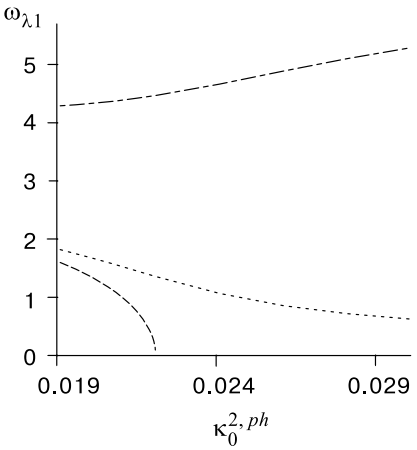

Fig. 5. The dependence of the $\omega_{\lambda 1}$ on $\kappa_0^{(2,ph)}$ in ^{64}Zn. The dashed line corresponds to the RPA result for $\lambda = 2$; the dotted line — to ERPA for $\lambda = 2$; the dot-dashed line — to ERPA $\lambda = 3$

Let us discuss in more detail the behaviour of the transition charge densities. Figure 7 shows the experimental [50] and calculated transition charge densities from the ground to the first 2^+ states in the ^{64}Zn. Our calculations for the $\rho_\nu^J(r)$ give results which are similar to the ones of [51], obtained in the RPA with the Skyrme forces, but in contrast with [51] we did not assign occupation probability to each single-particle orbital empirically. As was pointed in [51], the authors were enforced to destroy the self-consistency shifting the single-particle spectrum for the unoccupied orbitals with respect to the occupied ones to reproduce the experimental value for the first 2^+ state.

As one can see from Fig. 7 the RPA reproduces the behaviour of the transition charge densities qualitatively but it overestimates the interior part of the $\rho_\nu^J(r)$. The inclusion of the GSC beyond the RPA gives a 37% depletion of the maximum of the $\rho_\nu^J(r)$ in the interior region of the nucleus. The calculated $\rho_\nu^J(r)$ for ^{64}Zn becomes closer to the experimental data. Such a depletion is related with the Pauli blocking effect for the proton two-quasiparticle configuration $\{2p_{3/2}, 2p_{3/2}\}$, which is mainly responsible for the interior bump in the charge

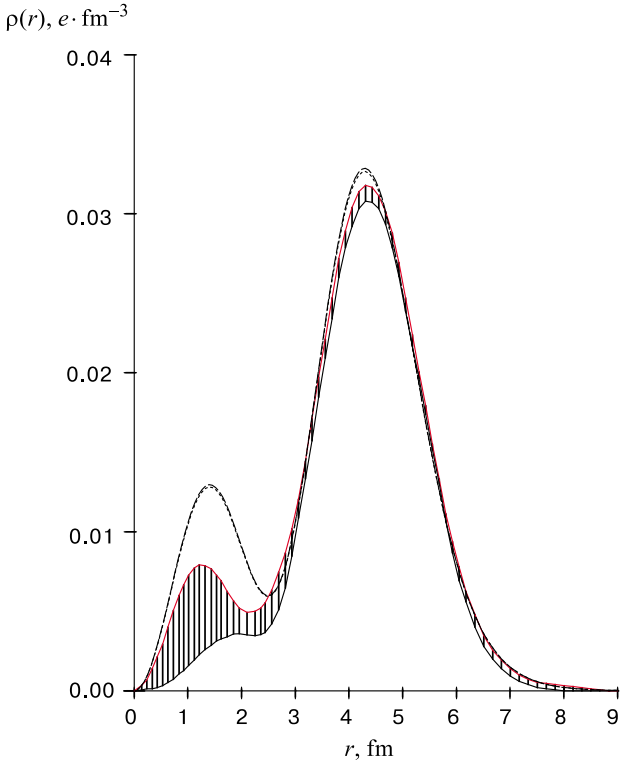

Fig. 6. The transition charge density from the ground to the first 2^+ state in ^{64}Zn. The dashed line corresponds to the ERPA result taking into account the p-h channel only; the dotted line — to the ERPA taking into account the p-h and p-p channels. Experimental data are presented by a shadowed area

transition densities in the Zn isotopes. According to our RPA calculations the proton two-quasiparticle configuration $\{2p_{3/2}, 2p_{3/2}\}$ gives a contribution about 24% into the norm of the first quadrupole phonon in ^{64}Zn. The inclusion of the GSC redistributes the strength of this configuration over many phonon roots and as a result the contribution into the first root becomes 18.1%. As follows from Eq. (3.33) the GSC suppresses the contribution of the partial two-quasiparticle transition densities having big $q_{jj'}$. It is seen from Table 1 that the $q_{2p_{3/2}}$ is the biggest for protons and as it was mentioned above plays an essential role in the structure of the interior part of the transition density for the 2^+_1 states. The configuration $\{1f_{5/2}, 1f_{5/2}\}$ gives some contribution in the interior part, too, and the same mechanism of a suppression takes place for it. Besides the blocking effect there are changes in the coefficients $u^{(+)}_{j_1 j_2}$ because of the influence of the

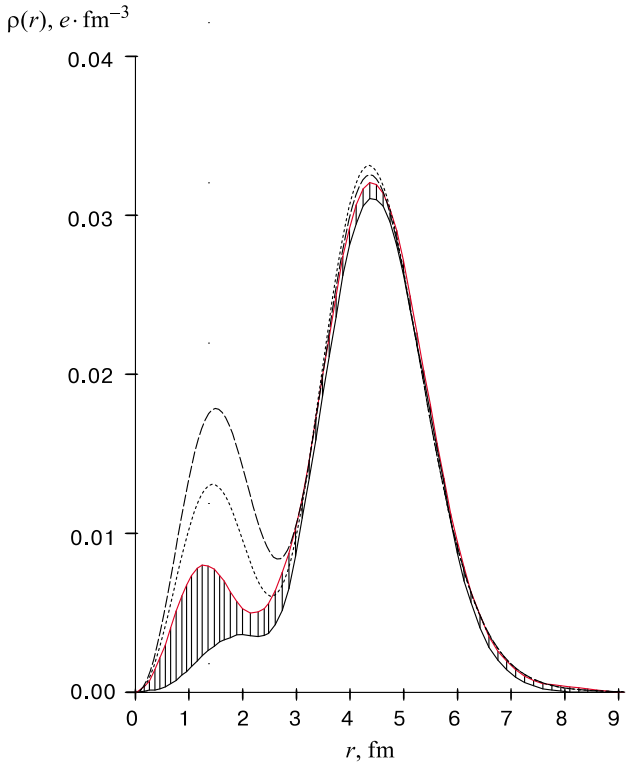

Fig. 7. The transition charge density from the ground to the first 2^+ state in ^{64}Zn. The dashed line corresponds to the RPA result; the dotted line — to ERPA. Experimental data are presented by a shadowed area

GSC on pairing and in the phonon amplitudes. All these effects suppress the interior bump. It should be noted that the amplitudes of the oscillations for the configurations with low orbital momenta are bigger than for the ones with high orbital momenta. That is, because the single particle wave functions with low orbital momenta are mainly localized in the interior part of nuclei in contrast to those with high orbital momenta.

The behaviour of the neutron transition densities differs from the proton ones (see Fig. 8). In the case of ^{64}Zn, for example, the influence of the GSC on the interior part of the transition density is very weak because the neutron configuration $\{2p_{3/2}, 2p_{3/2}\}$ contributes not more than 5% in the norm of the 2^+_1 state, and the contribution of the configuration $\{1f_{5/2}, 1f_{5/2}\}$ remains practically the same in all cases.

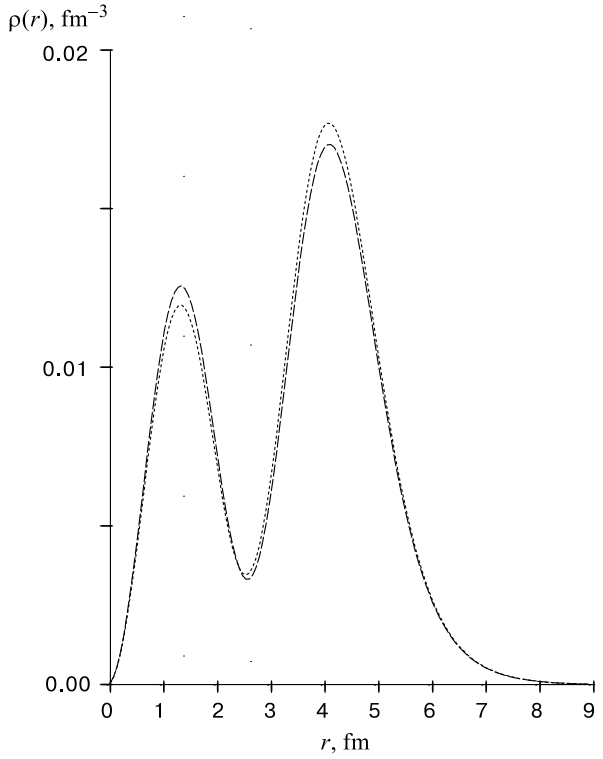

Fig. 8. The neutron transition density from the ground to the first 2^+ state in ^{64}Zn. The dashed line corresponds to the RPA result; the dotted line — to ERPA

We calculated the charge transition density for the one-phonon 4^+ state and did not find any essential oscillations in the interior region. That is due to the lack of the configuration $\{2p_{3/2}, 2p_{3/2}\}$ in such states because of the angular momentum coupling rule.

Figure 9 presents the charge transition density for the 3_1^- state in ^{64}Zn. This density has a clear surface nature and there are no strong oscillations in the interior region of the nucleus because of a destructive interference of the two-quasiparticle partial transition densities constructed from the single-particle wave functions with different parity. The same picture takes place in the other Zn isotopes and it is typical for the transition densities of the octupole vibration states (see Refs. 44–47).

It is interesting to note that the GSC increase slightly the ground state r.m.s. charge radii in comparison with its RPA values.

To study the influence of the GSC on the quasiparticle-phonon coupling we calculated the structure of the low-lying states in ^{68}Zn with the wave function

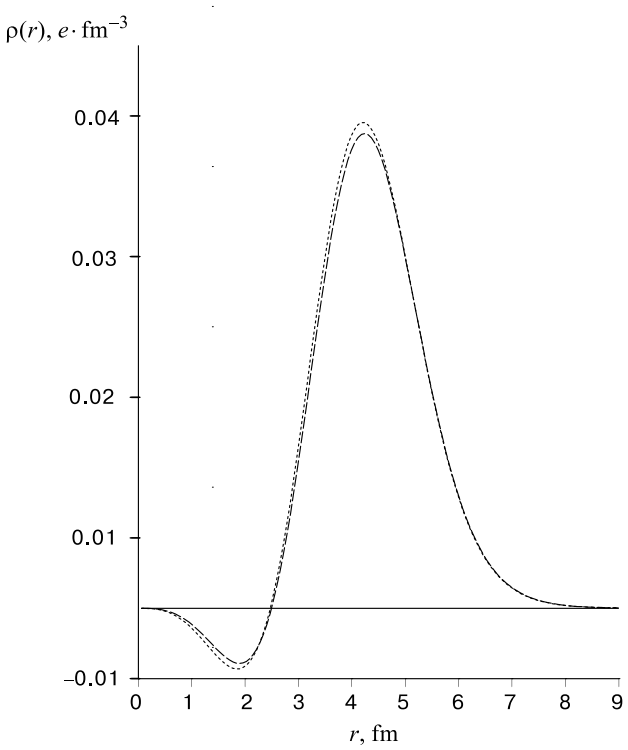

Fig. 9. The transition charge density from the ground to the first 3^- state in ^{64}Zn. The dashed line corresponds to the RPA result; the dotted line — to ERPA

(3.24). Experimental data [50, 52] and results of our calculations for the $2^+_{1,2}$ and 3^-_1 states within different approaches are shown in Table 2.

One can see from Table 2 that the RPA and ERPA overestimate the energies and fail to reproduce the transition probabilities for the 2^+_2 and 3^-_1 states. Taking into account coupling of the one- and two-phonon components improves essentially the description of all states under consideration. Besides the transitions to the ground state, one can reproduce the B(E2) value for the E2-transition between the first and the second 2^+ states. The inclusion of the Pauli principle corrections in two-phonon terms changes to worse the description of the second 2^+ state mainly. The EQPMPP describes energies and transition probabilities better than the QPMPP. It is worth to point out that the B(E2) values for the E2 transition between the first and the second 2^+ states depend essentially on the two-phonon components of the wave function of the 2^+_2 state and the latter can be affected by the three-phonon terms, which are out of the present consideration. One can conclude that the most consistent approach from theoretical point of

Table 2. Energies and B(Eλ)-values for up-transitions to some first vibrational states of ^{68}Zn

State	2_1^+		2_2^+		3_1^-	
	Energy	B(E2)	Energy	B(E2)	Energy	B(E3)
		$0^+ \to 2_1^+$		$0^+ \to 2_2^+$ $2_1^+ \to 2_2^+$		$0^+ \to 3_1^-$
	(MeV)	(e^2fm^4)	(MeV)	(e^2fm^4)	(MeV)	(e^2fm^6)
EXP.	1.077	1266	1.883	46 287	2.751	38400
RPA	1.360	1290	2.390	75	3.830	48240
QPM	1.090	1200	2.060	48 231	2.760	38550
QPMPP	1.140	1220	2.180	27 351	2.840	39200
ERPA	1.330	1250	2.320	106	3.980	43070
EQPM	1.080	1170	1.810	47 212.	2.760	34700
EQPMPP	1.080	1270	1.960	38 436	2.750	35660

view (EQPMPP), where the Pauli principle is taken into account in both one- and two-phonon terms, gives a rather good description of experimental data in general.

The transition probabilities are the integral characteristics of the vibrational states and they are less sensitive to the details of the nuclear wave functions than the differential ones. As was discussed above, the GSC affect essentially the charge transition densities. To test the developed approach we calculated the charge transition densities using Eq. (3.33) in ^{68}Zn within different approaches. Figures 10 and 11 show the transition charge densities ($\rho_\nu^{(J)}(r)$) from the ground to the first 2^+ state in ^{68}Zn. The experimental data [50] are presented as a shadowed area. Figure 10 shows results of calculations based on the RPA phonons while calculations based on the ERPA phonons are presented in Fig. 11.

The RPA reproduces the behaviour of the charge transition densities qualitatively, but it overestimates the interior part of the $\rho_1^{(2)}(r)$. As one can see from Fig. 10, the inclusion of the two-phonon terms (see the QPM case) reduces the bump in the interior part of $\rho_1^{(2)}(r)$ by 17%. This is due to the reduction of the

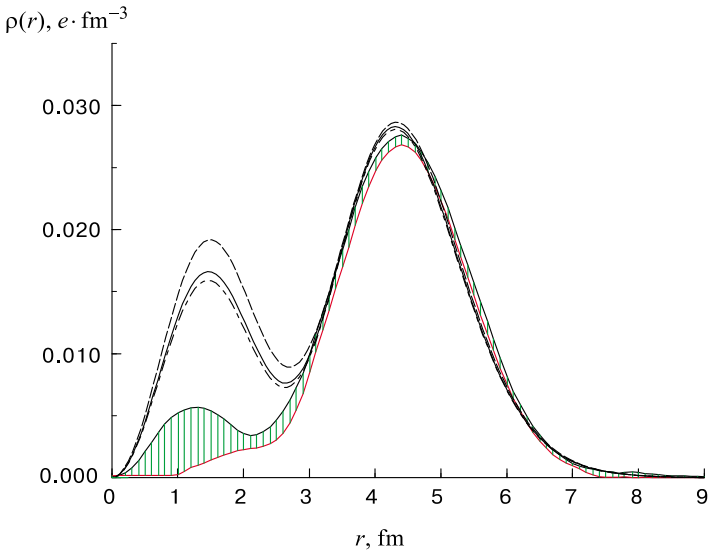

Fig. 10. The transition charge density from the ground to the first 2^+ state in ^{68}Zn. The dashed line corresponds to the RPA result; the dot-dashed line — to QPM; the full line — to QPMPP. Experimental data are presented by a shadowed area

contribution of the first term in Eq. (3.33) ($R_i < 1$). In spite of the dominance of the first term, the second one gives an additional reduction of ρ, too. The Pauli principle correction for the two-phonon terms (QPMPP case) changes results not more than by 3%.

Taking into account GSC beyond the RPA results in a suppression of interior oscillations by 9% in comparison with the RPA case (see Fig. 11). Such a depletion is related with the same Pauli blocking effects as it was discussed for ^{64}Zn. Taking into account the phonon coupling we get an additional lowering of the interior bump in the charge transition density and a reason of such lowering is the same as it was discussed above for the coupling of the RPA phonons. Finally the EQPM approach gives 30% reduction of the $\rho_1^{(2)}(r)$ in the interior nucleus region. It is worth to note that the Pauli principle corrections in two-phonon terms change the results slightly, but such corrections must be taken into account because they are often responsible for the weak electromagnetic transitions between excited states. One can see from Eq. (3.34) that the outer part of the charge transition density is responsible mainly for the value of the reduced transition probability. Since all above discussed approaches have very close values for this part of the charge transition density, the calculated B(E2) are close, too.

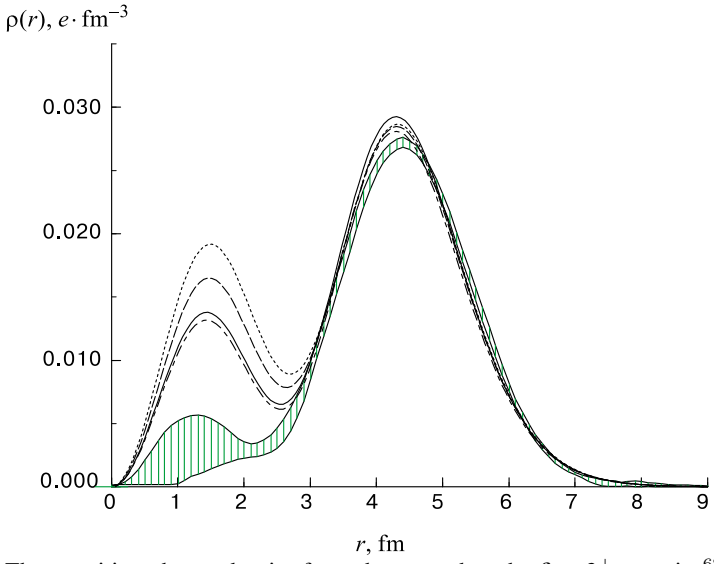

Fig. 11. The transition charge density from the ground to the first 2^+ state in ^{68}Zn. The dotted line corresponds to the RPA result; the dashed line — to ERPA; the dot-dashed line — to EQPM; the full line — to EQPMPP. Experimental data are presented by a shadowed area

We would like to emphasize that the depletion effect discussed above cannot be reproduced by any renormalization of the force strength $\kappa^{(2,ph)}$ in the RPA if one wants to describe energies and reduced transition probabilities. As concerning the charge transition density for the second 2^+ state, it is impossible to treat it without taking into account the three-phonon terms, which are out of the present consideration due to its numerical complexity.

The charge transition densities for the 3^-_1 states in all Zn isotopes have a clear surface nature and there are no strong oscillations in the interior region of the nucleus because of a destructive interference of the 2-qp partial transition densities constructed from the single-particle wave functions with different parity.

4. CONCLUSION

We have proposed a method to determine selfconsistently the one-body density matrix and the particle-hole excitations of a finite Fermi system without pairing. This method enables one to go beyond RPA avoiding the use of the quasiboson approximation, which can be questionable when the single particle occupation numbers deviate appreciably from their HF limiting values, namely 0 and 1.

Considering collective operators $Q_\nu^\dagger$ expressed as superpositions of p-h creation and annihilation operators and by using the equation-of-motion method, a set of RPA-like equations for the ψ and ϕ amplitudes defining the $Q_\nu^\dagger$'s and for the one-phonon energies has been obtained. The linearization is performed with respect to the correlated ground state. These equations, depending on the one-body density matrix, which in turn can be expressed in terms of the ψ and ϕ's, have been solved iteratively.

We have calculated spectra and strength distributions of some metallic clusters within the jellium approximation and with a pure Coulomb jellium-electron and electron-electron interaction. These calculations show that the new proposed method gives a better agreement with experiments than RPA. In particular there is a shift of the position towards lower energies with respect to RPA. This is partially due to the fact that in the new equations the one-body energy terms are no more the single particle HF energies.

A consistent treatment of the ground state correlations beyond the RPA including their influence on the pairing and phonon-phonon coupling in nuclei is presented. A new general system of nonlinear equations for the quasiparticle phonon model is derived. It is shown that this system contains as a particular case all equations derived for the QPM early. The system is solved numerically for the first time in a realistic case for Zn isotopes to study the effect of the GSC on the excitation energies, transition probabilities and charge transition densities of the vibrational states. Taking into account the GSC results in better agreement with experimental data for the characteristics of the low-lying states.

The GSC effect in the finite fermionic systems should be taken into account to treat correctly any physical value that includes matrix elements containing wave functions of levels near the Fermi surface.

5. ACKNOWLEDGEMENTS

We are thankful to Prof. V.G.Soloviev for many fruitful and stimulating discussions concerning various aspects of this work. We thank our colleagues M.Grasso, M.Grinberg, N. Van Giai, G.Piccitto and M.Sambataro for fruitful collaboration. This work has been partially supported by the Bulgarian National Science Foundation under contract Φ–621. Two of us (D.K. and V.V.V.) thank the INFN for the hospitality and support during their stay in Catania, where a part of this work was done.

REFERENCES

1. **Rowe D.J.** — Revs. Mod. Phys., 1968, v.40, p.153.
2. **Sambataro M., Catara F.** — Phys. Rev., 1995, v.C51, p.3066.

3. **Hara K.** — Progr. Theor. Phys., 1964, v.32, p.88.
4. **Ikeda K., Udagawa T., Yamaura H.** — Prog. Theor. Phys., 1965, v.33, p.22.
5. **da Providencia J.** — Nucl. Phys., 1968, v.A108, p.589.
6. **Schuck P., Ethofer S.** — Nucl. Phys., 1973, v.A212, p.269;
Dukelsky J., Schuck P. — Nucl. Phys., 1990, v.A512, p.466.
7. **Jolos R.V., Rybarska W.** — Z. Physik, 1980, v.A296, p.73.
8. **Nawrocka-Rybarska W., Stoyanova O., Stoyanov Ch.** — Yad. Fiz., 1980, v.33, p.1494.
9. **Lenske H., Wambach J.** — Phys. Lett., 1990, v.B249, p.377.
10. **Klein A., Walet N.R., Do Dang G.** — Nucl. Phys., 1991, v.A535, p.1.
11. **Karadjov D., Voronov V.V., Catara F.** — Phys. Lett., 1993, v.B306, p.197.
12. **Karadjov D., Voronov V.V., Catara F.** — J. Phys., 1994, v.G20, p.1431.
13. **Karadjov D., Voronov V.V., Catara F., Grinberg M., Severyukhin A.P.** — Nucl. Phys., 1998, v.A643, p.259.
14. **Catara F., Dinh Dang N., Sambataro M.** — Nucl. Phys., 1994, v.A579, p.1.
15. **Catara F., Piccitto G., Sambataro M., Van Giai N.** — Phys. Rev., 1996, v.B54, p.17 536.
16. **Catara F., Grasso M., Piccitto G., Sambataro M.** — Phys. Rev., 1998, v.B58, p.16 070.
17. **Toivanen J., Suhonen J.** — Phys. Rev., 1997, v.C55, p. 2314.
18. **Hirsch J.G., Hess P.O. Civitarese O.** — Phys. Rev., 1997, v.C56, p.199.
19. **Raduta A.A., Raduta C.M., Faessler A., Kaminski W.A.** — Nucl. Phys., 1998, v.A654, p.497.
20. **Vdovin A.I., Kosov D.S., Nawrocka W.** — Theor. Math. Phys., 1997, v.111, p.613.
21. **Storozhenko A.N., Vdovin A.I.** — Eur. Phys. J., 1999, v.5, p.263.
22. **Severyukhin A.P., Voronov V.V., Karadjov D.** — JINR Preprint P4-99-121, Dubna, 1999.
23. **Vdovin A.I., Soloviev V.G.** — Phys. of Part. & Nucl., 1983, v.14, p.99.
24. **Voronov V.V., Soloviev V.G.** — Phys. of Part. & Nucl., 1983, v.14, p.583.
25. **Vdovin A.I., Voronov V.V., Soloviev V.G., Stoyanov Ch.** — Phys. of Part. & Nucl., 1985, v.16, p.245.
26. **Soloviev V.G.** — Theory of Atomic Nuclei: Quasiparticles and Phonons. Institute of Physics, Bristol and Philadelphia, 1992.
27. **Yannouleas C., Catara F., Van Giai N.** — Phys. Rev., 1995, v.B51, p.4569.
28. **Catara F., Serra L.I., Van Giai N.** — Zeit. Phys., 1997, v.D39, p.153.
29. **Ring P., Schuck P.** — The Nuclear Many-Body Problem. Springer, New York, 1980.
30. **Rowe D.J.** — Phys. Rev., 1968, v.175, p.1283.
31. **Sanderson E.A.** — Phys. Lett., 1965, v.19, p.141.
32. **Toivanen J., Suhonen J.** — Phys. Rev. Lett., 1995, v.75, p.410.
33. **Pines D., Nozières Ph.** — The Theory of Quantum Liquids, vol.1. Benjamin, New York, 1966.
34. **Kresin V.V.** — Phys. Rep., 1992, v.220, p.1.
35. **de Heer W.A.** — Rev. Mod. Phys., 1993, v.65, p.611.
36. **Bohr A., Mottelson B.** — Nuclear Structure, vol.2. Benjamin, New York, 1975.
37. **Voronov V.V., Soloviev V.G.** — Theor. Math. Phys., 1983, v.57, p.75.

38. **Karadjov D., Voronov V.V., Catara F.** — In Proc. of 5th Int. Spring Seminar on Nuclear Structure, Ravello 1995, World Scientific, Singapore, 1996, p. 215.

39. **Voronov V.V., Karadjov D.** — Frontiers in Nuclear Physics. JINR, D4-95-308, Dubna, 1995, p.273.

40. **Bertsch G.F., Tsai S.F.** — Phys. Rep., 1975, v.C18, p.125.

41. **Fayans S.A., Khodel V.A., Saperstein E.E.** — Nucl. Phys., 1979, v.A317, p.424.

42. **Heisenberg J. et al.** — Phys. Rev., 1984, v.C25, p.2292.

43. **Broglia R.A., Barranco F., Gallardo F.** — Nuclear Structure 1985, ed. by R.A. Broglia, G.B. Hagemann and B. Herskind, Elsevier Science Publishers B.V., 1985, p.193.

44. **Sandor R.K.J. et. al.** — Nucl. Phys., 1991, v.A535, p.669.

45. **Kim W. et al.** — Phys. Rev., 1991, v.C44, p.2400.

46. **Heisenberg J., Block H.P.** — Ann. Rev. Nucl. Part. Sci., 1983, v.33, p.569.

47. **Frois B., Papanicolas C.N.** — Ann. Rev. Nucl. Part. Sci., 1987, v.37, p.133.

48. **Simon G.G. et al.** — Nucl. Phys., 1980, v.A333, p.381.

49. **Satchler G.R.** — Direct Nuclear Reactions, New York–Oxford Univ. Press, 1983.

50. **Neuhausen R.** — Nucl. Phys., 1977, v.A282, p.125.

51. **Tsai S.F., Bertsch G.F.** — Phys. Lett., 1975, v.B59, p.425.

52. **De Vries H. et al.** — Atomic Data and Nucl. Data Tables, 1987, v.36, p.495.